

FRONTOGENETIC REGIONS IN THE FAR EAST

Thesis

by

Hsia-Chien Huang.

In Partial Fulfillment of the Requirements  
for the Degree of Doctor of Philosophy,  
California Institute of Technology,  
Pasadena, California, 1937.

## CONTENTS

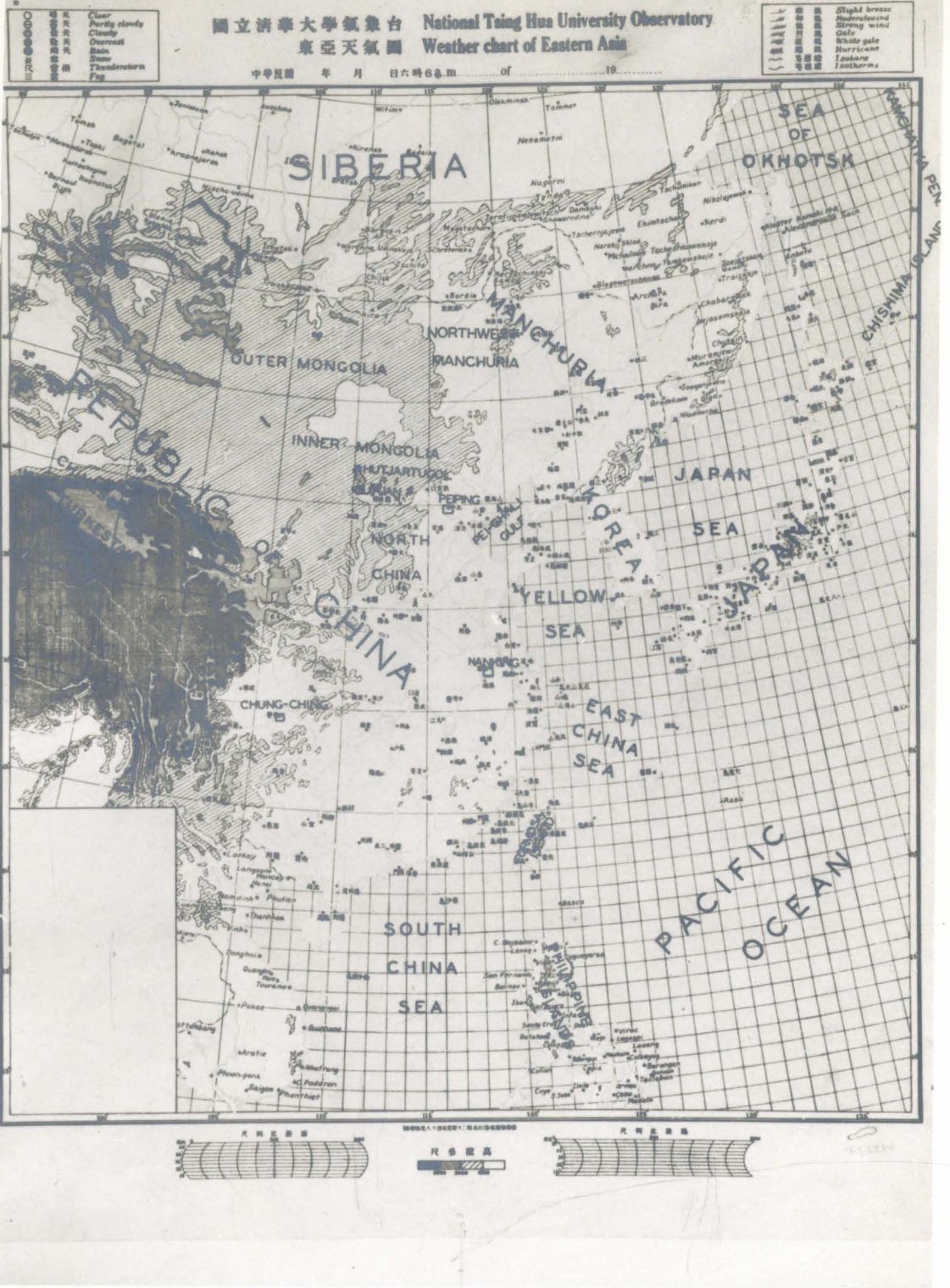
Summary	1
I. Introduction	1
II. Mathematical and Physical Aspects of the Field of Motion	3
III. Frontogenesis in a Field of Motion	9
IV. Sources and Treatment of Material	16
V. Air Masses and Field of Motion in the Far East	20
VI. Frontogenetic Regions in the Spring Season	26
VII. Frontogenetic Regions in the Summer Season	32
VIII. Frontogenetic Regions in the Autumn Season	42
IX. Frontogenetic Regions in the Winter Season	49
X. Acknowledgement	57
References	58
Charts	61-88

## LIST OF CHARTS

MAP OF THE FAR EAST	Frontispiece
CHART I      Deformation Fields and Isotherms-April	P.27
II      Wind Directions over China-April	"
III      v<  Field in the Far East-April	29
IV      Distribution of F in the Far East-April	"
V      Frontogenetic Lines and Cyclonic Tracks in the Far East-April	30
VI      Deformation Fields and Isotherms-July	34
VII      v<  Field in the Far East-July	"
VIII     Distribution of F in the Far East-July	"
IX      Frontogenetic Lines and Cyclonic Tracks in the Far East-July	"
X      Synoptic Chart of August 19, 1932	40
XI      "      "      "      "      20,      "	"
XII     "      "      "      "      21,      "	"
XIII    "      "      "      "      22,      "	"
XIV     Deformation Fields and Isotherms-September	43
XV      v<  Field in the Far East-September	45
XVI     Distribution of F in the Far East-September	"
XVII    Frontogenetic Lines and Cyclonic Tracks in the Far East-September	46
XVIII   Deformation Fields and Isotherms-January	49

CHART XIX	Field in the Far East-January	P.50
XX	Distribution of P in the Far East- January	50
XXI	Frontogenetic Line and Cyclonic Activity- January	51
XXII	Synoptic Chart of January 15, 1933	54
XXIII	" " " " 16, "	"
XXIV	" " " " 17, "	"
XXV	Deformation Field and Isotherms-January 16, 1933	55
XXVI	Deformation Field and Isotherms-January 17, 1933	"
XXVII	Synoptic Chart of January 18, 1933	"

# MAP OF THE FAR EAST



## Summary

The general field of motion of the atmosphere in the Far East is a deformation type with the deformation axis in a NE-SW direction which orients the frontogenetic lines of the Far East to run in that same direction along the Asiatic coast at varying distances from it. The actual position of the lines is different in different seasons and is dependent upon the seasonal activity of the two anticyclones, the Pacific High and the Siberian High, which actually control the field of motion of the region. Due to the preponderant activity of the Pacific High and the Siberian High in the summer and winter respectively there is only one frontogenetic line found for each of these two seasons. In the other seasons there are two lines, one offshore and one inland. All the frontogenetic lines determined by the frontogenetic theory are essentially in agreement with the actual frontal activity in the region shown by the observed cyclone tracks.

The region from the Formosa Strait northeastward to the Japanese Islands is specifically frontogenetic for most seasons of the year while the land area of the northern part of China is only effectively frontogenetic in the summer season. The difference in orientation of the isotherms between the two mentioned regions is the main reason for this fact.

Winter cyclones in the Far East take place at a cold front between two types of air masses of Ps origin, not between Ps and true Tp. They are developed from wave perturbations.

Typhoons are formed dynamically at the line of convergence between the Equatorial Pacific and the Tropical Pacific air masses at the southwest corner of the North Pacific Ocean. The location of forming and trajectories conform with the position of this line.

FRONTOGENETIC REGIONS IN THE FAR EAST

I.

Introduction

First, we know that in the atmosphere various types of air masses (M) exist. Usually the difference of potential temperature( $\theta$ ) between dissimilar types must exceed  $10^{\circ}\text{C}$  before they can be classified as distinct masses. When one mass moves closer to ~~an~~ another mass, as their potential temperatures are different, an increase in the value of  $\frac{\partial\theta}{\partial x}$  and  $\frac{\partial\theta}{\partial y}$  will occur and finally a rapid transition zone will arise between them. The masses in this case are, according to T. Bergeron, (1) called the "Frontalmasse" or the Frontal Masse and the zone the "Frontalzone" or the Frontal Zones. These two names can be further grouped into a simple abbreviation of FM. Once a Frontal Zone has been formed any further development will quickly intensify the zone into a real Front (F). This is the fundamental idea of front formation. Thus the process is:  $M \rightarrow FM \rightarrow F$ . Any other process of front formation, such as by heating the air on one side and cooling on the other side, would be a minor one. The reverse process of front destruction would of course be the reverse, i.e.  $F \rightarrow FM \rightarrow M$ .

The idea of air masses and air mass boundaries or fronts between the dissimilar types has been brought down first from W. Koppen's work in 1879-1882 (2). Dove, Blasius, and Helmholtz from purely theoretical consideration arrived at their believe that discontinuity surface must exist between the cold northern

currents and the warm southern currents. Later on Ficker, Fessler and Exners studied the occurrence of the migrating cold waves which actually are the material proof of the existence of cold fronts at the earth's surface. However, the immediate attack on the problem of front formation has only been made in very recent years. T. Bergeron first introduced the use of the term "Frontogenese" or Frontogenesis for front formation and "Frontolyse" or Frontolysis for front destruction. By frontogenesis is meant the formation of a new front or the intensification of preexistent front. In both these cases the solenoids, the cells bounded by adjacent isobaric and isosteric surfaces, in the frontal zone are increased with the same change in the values of  $\frac{\partial\theta}{\partial x}$  and  $\frac{\partial\theta}{\partial y}$ . Therefore we can simply define Frontogenesis as a process which increases the number of solenoids or the values of  $\frac{\partial\theta}{\partial x}$  and  $\frac{\partial\theta}{\partial y}$ . The reverse is true for Frontolysis.

Frontogenesis can be dealt with by a two dimensional method or preferably by a three dimensional method. The later method is rather complicated for practical use. In the present study no attempt has been made to discuss the theoretical side in detail, but a practical determination of the frontogenetic regions in the Far East is desired. The method of the study will be limited to a two dimensional application. T. Bergeron's and Sverre Petterssen's ideas on frontogenesis will be the theoretical basis for the study, use being made generally of Petterssen's latest paper (3) and also his lectures at the California Institute of Technology, Pasadena, California, U.S.A., 1935.



II.

Mathematical and Physical Aspects of the  
Field of Motion

Supposing that the motions in the atmosphere are adiabatic, frontogenesis can be regarded as a purely kinematical process and from a field of motion we can easily discover the change in the distribution of a conservative property belonging to the air particles after a change of time  $t$ . In order to find a place where FG is likely to occur, it is necessary to introduce some concepts regarding two dimensional fields of motion. If  $u$  and  $v$  are the components of the velocity in the  $x$  and  $y$  direction respectively and they are each functions of  $x$  and  $y$  we will have:

$$(1) \quad u = u(x, y), \quad v = v(x, y).$$

Expanding these by Taylor's Series and neglecting the terms of higher orders we obtain:

$$(2) \quad \begin{aligned} u &= u_0 + \frac{\partial u}{\partial x} x + \frac{\partial u}{\partial y} y + \dots \\ v &= v_0 + \frac{\partial v}{\partial x} x + \frac{\partial v}{\partial y} y + \dots \end{aligned}$$

We may rewrite these equations as follows:

$$(3) \quad \begin{aligned} u &= u_0 + ax + by - cy \\ v &= v_0 - ay + by + cx \end{aligned}$$

the coefficients will have the following values:

$$(4) \quad \begin{aligned} a &= \frac{1}{2} \left( \frac{\partial u}{\partial x} - \frac{\partial v}{\partial y} \right) \\ b &= \frac{1}{2} \left( \frac{\partial u}{\partial x} + \frac{\partial v}{\partial y} \right) \\ c &= \frac{1}{2} \left( \frac{\partial v}{\partial x} - \frac{\partial u}{\partial y} \right) \end{aligned}$$

With these coefficients, equation (3) indicates four components of motion in a two dimensional field, namely, the first term is the translation ( $u_0, v_0$ ), second, the dilatation (+a) or contraction (-a), third, the divergence (+b) or convergence (-b) and fourth, the clockwise (or anti-cyclonic) rotation (-c) or counter-clockwise (or cyclonic) rotation (+c). The streamline pictures of translation are shown below:

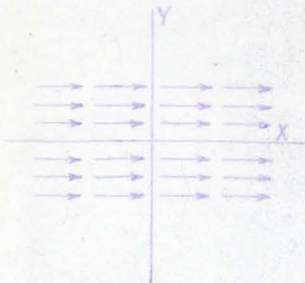


Fig.1

Field of  $u=u_0$ .

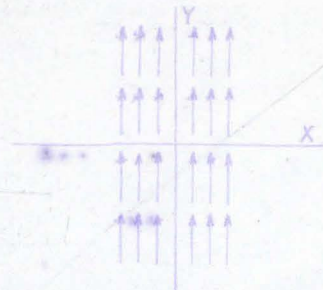


Fig.2

Field of  $v=v_0$ .

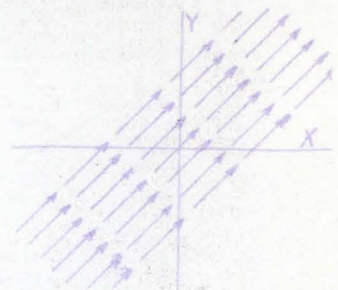


Fig.3

Combined field

A glance on the above stream line pictures shows that there is no tendency to bring one particle nearer to another particle. This kind of motion, therefore, has no influence on FG, but will merely distort the original configuration of an  $\alpha$ -line field to a new configuration when the motion is superimposed.

For the second term, when (a) is positive, the stream line picture of  $u=ax$  is:

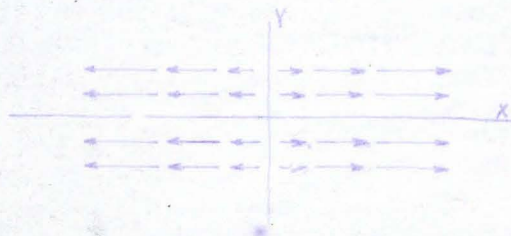


Fig.4 Field of  $u=ax$

Apparently, the motion is tending to destroy a front along the

Y-axis. When (a) is negative the stream picture of  $v = -ay$  will show the following result:

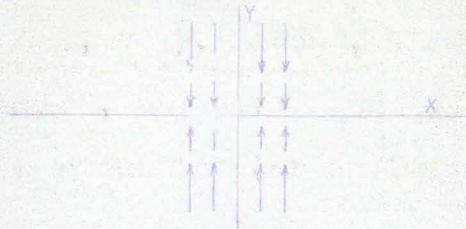


Fig.5 Field of  $v = -ay$

The Y component is then the effective one in FG along the X-axis. Combining the above fields, we obtain a stream line picture :

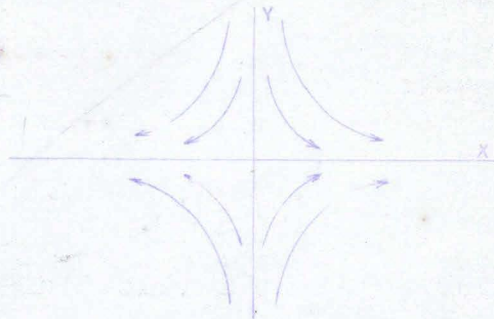


Fig.6 Combined field of  $u = ax$  and  $v = -ay$

The above picture shows a pure deformation field, and the X-axis in the combined field in this case is the axis of dilatation, also the deformation axis. (Note that if  $u = -ax$  and  $v = ay$ , Y becomes the deformation axis).

*and* The third term, when (b) is positive, the stream line pictures of  $u = bx$  and  $v = by$  show the motion of particles along the X and Y-axis with a separating tendency.

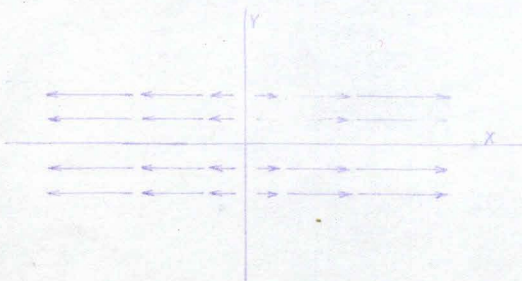


Fig.7

Field of  $u = bx$

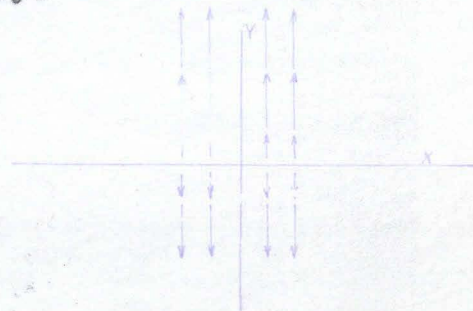


Fig.8

Field of  $v = by$

Combining the fields, we obtain a divergent flow and, of course, Frontolysis.

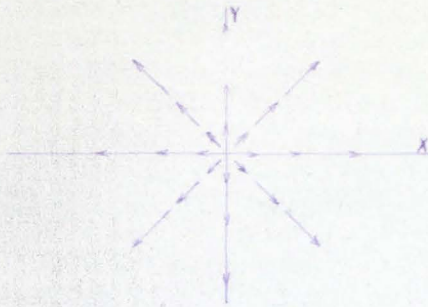


Fig.9

Combined field of  $u=bx$  and  $v=by$

Contrarily, when (b) is negative, the motion in the field will bring particles concentrating along the X and Y-axis and a convergent flow will be found by combining the fields.

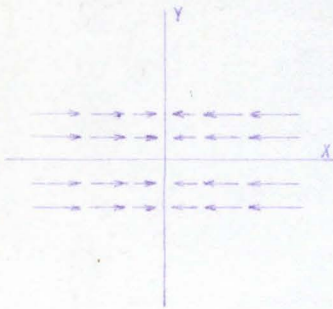


Fig.10

Field of  $u=-bx$

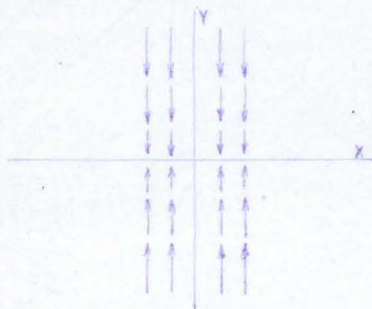


Fig.11

Field of  $v=-by$

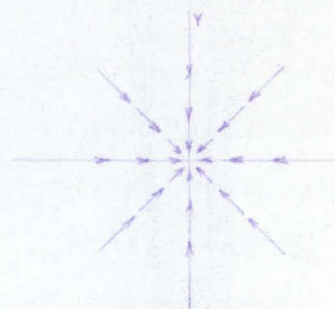


Fig.12

Combined field.

This is, theoretically, a very effective frontogenetic field.

The fourth term, since u is independent of x and v of y, gives a stream line picture of circular rotation with either clockwise (c being negative) or counter-clockwise (c being positive) direction.

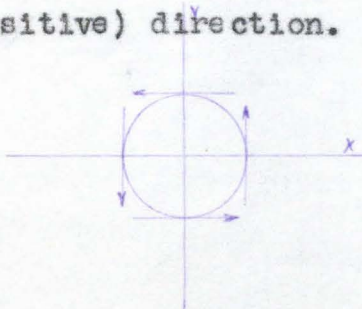


Fig.13

Field of  $v=cx$

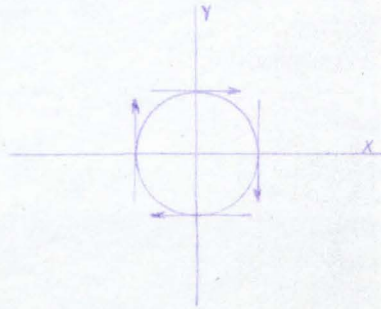


Fig.14

Field of  $u=-cy$

The motion will have no influence either on FG or FL as ~~is~~ there <sup>is</sup> no tendency to bring the particles closer or farther apart.

From the above four components of the field of motion many stream line patterns can be developed by superimposing them in various degrees of intensity. However, only a few patterns of central stream lines of hyperbolic type, that is to say  $b^2 < a^2 - c^2 > 0$ , will be of interest in this research problem because they are most often found in the Far East. The patterns are shown below:

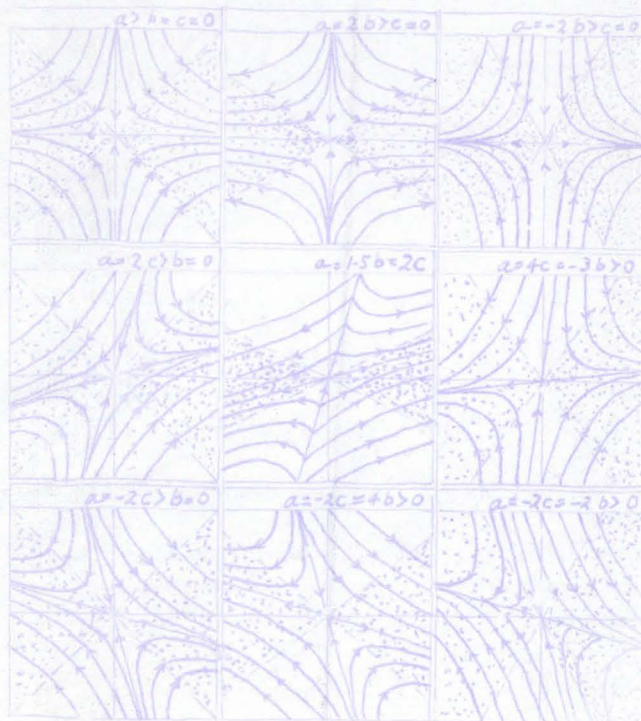


Fig.15

Hyperbolic stream lines when  $b^2 < a^2 - c^2 > 0$

(After Sverre Petterssen)

An actual field of curved stream lines without center, that is to say  $\frac{v_0}{u_0} > -\frac{b-a}{c} = -\frac{c}{b+a}$ , has also been found in the Far East, and will be discussed later.

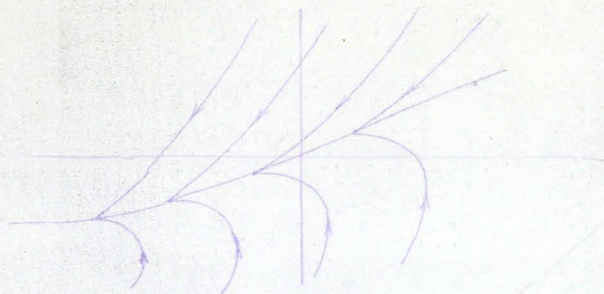


Fig. 16

Curved stream lines when  $\frac{v_0}{u_0} > -\frac{b-a}{c} = -\frac{c}{b+a}$

(After Sverre Pettersen)

III.

Frontogenesis in a Field of Motion

If a certain kind of velocity field be superimposed upon a given distribution of meteorological elements after a time  $t$  the new configuration of the distribution of meteorological elements must be the result of the motion of the field. Let  $\alpha$  be any conservative property such as potential temperature or specific humidity.

$$\alpha = \alpha(x, y, t)$$

Along a line of FG the  $\alpha$ -lines must approach each other more rapidly than in any portions of the field. We shall define  $-\nabla\alpha$  as the gradient of the  $\alpha$ -lines and  $-\nabla\alpha$  the magnitude of the gradient. In order to see what happens between two iso- $\alpha$  lines along a line normal to the line of FG, we may apply the well known transformation equation of hydrodynamics: (4)

$$\frac{\delta(\quad)}{\delta t} = \frac{\partial(\quad)}{\partial t} + \nabla \cdot \nabla(\quad)$$

choosing an axis normal to the line of FG. Putting  $|\nabla\alpha|$  in the symbolic equation, we have:

$$(5) \quad \frac{\delta|\nabla\alpha|}{\delta t} = \frac{\partial|\nabla\alpha|}{\partial t} + \nabla \cdot \nabla|\nabla\alpha|$$

where  $\frac{\delta|\nabla\alpha|}{\delta t}$  is the rate of the change of  $|\nabla\alpha|$  referred to a moving system of coordinates fixed to the line of FG,  $\frac{\partial|\nabla\alpha|}{\partial t}$  the rate of change of  $|\nabla\alpha|$  at a fixed station,  $\nabla$  the velocity of the line of FG. When the iso- $\alpha$  lines move together the value of  $|\nabla\alpha|$  is increased. Let  $F = \frac{\delta|\nabla\alpha|}{\delta t}$  which is an expression showing how quickly the iso- $\alpha$  lines move together. Therefore

we might call F the Frontogenetical Function. To have FG, F must be a maximum along a line normal to the line of FG or  $\frac{\partial F}{\partial N} = 0$  and  $\frac{\partial^2 F}{\partial N^2} < 0$ , N being the distance on the line normal to the line of FG. If  $\frac{\partial^2 F}{\partial N^2} > 0$ , a condition of FL would arise.

Taking the right hand side of equation (5), to solve for  $\frac{\partial \alpha}{\partial t}$  we know that  $\alpha = \alpha(x, y, t)$ . Differentiating totally with respect to t we obtain:

$$\begin{aligned}
 (6) \quad \frac{d\alpha}{dt} &= \frac{\partial \alpha}{\partial t} + \frac{\partial \alpha}{\partial x} \frac{dx}{dt} + \frac{\partial \alpha}{\partial y} \frac{dy}{dt} & \frac{dx}{dt} = u, \quad \frac{dy}{dt} = v \\
 &= \frac{\partial \alpha}{\partial t} + \frac{\partial \alpha}{\partial x} u + \frac{\partial \alpha}{\partial y} v & \frac{\partial \alpha}{\partial x} + \frac{\partial \alpha}{\partial y} = \nabla \alpha, \\
 &= \frac{\partial \alpha}{\partial t} + \nabla \cdot \nabla \alpha. & u+v = \nabla, \text{ the wind velocity.}
 \end{aligned}$$

Since  $\alpha$  is a conservative property, we can write:

$$(7) \quad \frac{d\alpha}{dt} = \frac{\partial \alpha}{\partial t} + \nabla \cdot \nabla \alpha = 0$$

$$\therefore (8) \quad \frac{\partial \alpha}{\partial t} = -\nabla \cdot \nabla \alpha.$$

The change of  $\frac{\partial \alpha}{\partial t}$  is:

$$(9) \quad \nabla \frac{\partial \alpha}{\partial t} = \frac{\partial \nabla \alpha}{\partial t} = -\nabla \nabla \cdot \nabla \alpha - \nabla \cdot \nabla \nabla \alpha.$$

Since  $\nabla \alpha$  is a vector we may write:

$$(10) \quad \frac{\partial \nabla \alpha}{\partial t} = \frac{\partial |\nabla \alpha|}{\partial t} n$$

where n denotes the direction of a vector and can be written

$$(11) \quad n = \frac{\nabla \alpha}{|\nabla \alpha|}.$$

Equation (9) becomes:

$$(12) \quad n \frac{\partial |\nabla \alpha|}{\partial t} = -\nabla \nabla \cdot \nabla \alpha - \nabla \cdot \nabla \nabla \alpha.$$

Multiplying (12) by (11), we have:

$$(13) \quad n \cdot n \frac{\partial |\nabla \alpha|}{\partial t} = \frac{\nabla \alpha}{|\nabla \alpha|} \cdot (-\nabla \nabla \cdot \nabla \alpha - \nabla \cdot \nabla \nabla \alpha) \quad n \cdot n = 1$$

$$\therefore (14) \quad \frac{\partial |\nabla \alpha|}{\partial t} = \frac{-\nabla \alpha \cdot \nabla \nabla \cdot \nabla \alpha - \nabla \alpha \cdot \nabla \cdot \nabla \nabla \alpha}{|\nabla \alpha|}$$

which gives the first term of equation (5).



The second term of the right hand side of equation (5) is  $\nabla \cdot \nabla |\nabla \alpha|$  which can be solved first by putting (15)  $\nabla \alpha = n |\nabla \alpha|$ . Multiplying this equation by (11), we obtain:

$$(16) \quad \frac{\nabla \alpha \cdot \nabla \alpha}{|\nabla \alpha|} = n \cdot n |\nabla \alpha|$$

$$(17) \quad \frac{\nabla \alpha \cdot \nabla \alpha}{|\nabla \alpha|} = |\nabla \alpha|$$

The variation of  $\frac{\nabla \alpha \cdot \nabla \alpha}{|\nabla \alpha|}$  is: (18)  $\nabla \frac{\nabla \alpha \cdot \nabla \alpha}{|\nabla \alpha|} = \nabla |\nabla \alpha|$ .

Expanding the left hand side of this equation, it becomes:

$$(19) \quad \frac{|\nabla \alpha| 2 \nabla \alpha \cdot \nabla \nabla \alpha - \nabla \alpha \cdot \nabla \alpha \cdot \nabla |\nabla \alpha|}{|\nabla \alpha|^2} = \nabla |\nabla \alpha|$$

$$(20) \quad \frac{2 \nabla \alpha \cdot \nabla \nabla \alpha}{|\nabla \alpha|} - \frac{\nabla \alpha \cdot \nabla \alpha}{|\nabla \alpha|^2} \nabla |\nabla \alpha| = \nabla |\nabla \alpha|$$

where  $\frac{\nabla \alpha \cdot \nabla \alpha}{|\nabla \alpha|^2}$  is equal to  $\frac{\nabla \alpha}{|\nabla \alpha|} \cdot \frac{\nabla \alpha}{|\nabla \alpha|}$  or, by equation (11), equal to  $n \cdot n$ , i.e., 1. Therefore, equation (20) becomes:

$$(21) \quad \frac{2 \nabla \alpha \cdot \nabla \nabla \alpha}{|\nabla \alpha|} - \nabla |\nabla \alpha| = \nabla |\nabla \alpha|$$

$$(22) \quad \frac{2 \nabla \alpha \cdot \nabla \nabla \alpha}{|\nabla \alpha|} = 2 \nabla |\nabla \alpha| \quad \therefore (23) \quad \nabla |\nabla \alpha| = \frac{\nabla \nabla \alpha \cdot \nabla \alpha}{|\nabla \alpha|}$$

Substituting equation (14) and (23) into the right hand side of equation (5), we obtain:

$$(24) \quad \frac{\delta |\nabla \alpha|}{\delta t} = F = \frac{-\nabla \alpha \cdot \nabla \nabla \alpha - \nabla \alpha \cdot \nabla \cdot \nabla \nabla \alpha}{|\nabla \alpha|} + \nabla \frac{\nabla \nabla \alpha \cdot \nabla \alpha}{|\nabla \alpha|}$$

Finally, (25) 
$$F = \frac{-\nabla \alpha \cdot \nabla \nabla \alpha - \nabla \alpha \cdot \nabla \cdot \nabla \nabla \alpha (\nabla - \nabla)}{|\nabla \alpha|}$$

Since  $\alpha$  is conservative so that  $\nabla$  is necessarily equal to  $\nabla$ .

We may write: (26) 
$$F = - \frac{\nabla \alpha \cdot \nabla \nabla \cdot \nabla \alpha}{|\nabla \alpha|}$$

In the foregoing equation  $-\nabla \alpha$  is the gradient of the iso- $\alpha$  lines, while  $\frac{\nabla \alpha}{|\nabla \alpha|}$  is the unit vector of  $\nabla \alpha$ . The vector  $\frac{\nabla \alpha}{|\nabla \alpha|} \cdot \nabla \nabla$  gives the variation in  $\nabla$ , the wind velocity along the vector lines of  $\nabla \alpha$ . Equation (26) shows that the frontogenetical function is the product of the gradient of the iso- $\alpha$  lines multiplied by this last vector. Since the gradient of iso- $\alpha$  lines is a vector so we may use  $r$  for the unit in the direction of  $\nabla \alpha$  and write  $\nabla \alpha = r \cdot |\nabla \alpha|$ . Rewriting equation (26) then

becomes: (27) 
$$F = \frac{-\nabla\alpha \cdot \nabla\nabla \cdot \nabla\alpha}{|\nabla\alpha|} = -(\gamma \cdot \nabla\nabla) \cdot \gamma |\nabla\alpha|.$$

Putting  $\gamma = mi + nj$ , we obtain:

where:-  $\frac{\partial u}{\partial x} = a+b$  (2,3)

(28) 
$$F = -(mi+nj) \cdot \nabla\nabla \cdot (mi+nj) |\nabla\alpha|$$

$\frac{\partial u}{\partial y} = -c$  "

(29) 
$$= -(m^2 \frac{\partial^2 u}{\partial x^2} + mn \frac{\partial^2 u}{\partial y^2} + mn \frac{\partial^2 v}{\partial x^2} + n^2 \frac{\partial^2 v}{\partial y^2}) |\nabla\alpha|$$

$\frac{\partial v}{\partial x} = c$  "

$\frac{\partial v}{\partial y} = b-a$  "

(30) 
$$= -\{m^2(a+b) + n^2(b-a)\} |\nabla\alpha|$$

$m^2 + n^2 = 1$

(31) 
$$= -\{b+a(m^2-n^2)\} |\nabla\alpha|.$$

The following diagram shows the distribution of the iso- $\alpha$  lines in a field of motion where the X-axis has been chosen as the axis of deformation and  $\phi$  taken as the angle between the line tangent to the iso- $\alpha$  lines and the X-axis. The distance h is the perpendicular to the iso- $\alpha$  lines and  $|\nabla\alpha|$

Fig. 17.

is equal to  $1/h$ . In this way we can substitute for  $m = -\sin \phi$  and  $n = \cos \phi$  in the last equation and get:

(32) 
$$F = (a \cos 2\phi - b) |\nabla\alpha|.$$

This equation becomes useful in calculating the value of F, the frontogenetical function, from an iso- $\alpha$  line field superimposed on a field of motion. Obviously if b in the equation is negligible, the angle  $\phi$  cannot be larger than  $45^\circ$  otherwise F will be negative and frontolysis will arise.

This is exactly true in the case of pure deformation fields when  $b=0$ .

For other fields the sign of  $F$  is dependent upon whether the line of iso- $\alpha$  is in the frontogenetic or frontolytic sector. This term, frontogenetical sector is used to designate the region bounded by two lines of  $F=0$ , on either side of a dilatation axis (which may not coincide with the X-axis). Since when  $F=0$ , we can solve  $\cos 2\phi = \frac{b}{a}$  to get the angle between these two lines,  $2\phi'$ , or the angle of the frontogenetical sector. Petterssen uses  $2\phi'$  for this angle and calls it the frontogenetical angle, as determined by  $\frac{b}{a}$  to avoid confusion with the measured angle  $\phi$  which remains the angle between the iso- $\alpha$  lines and the deformation axis. This latter angle if smaller than  $\phi'$  indicates that the iso- $\alpha$  lines fall in the frontogenetic sector and  $F$  is naturally positive. The smaller the angle  $\phi$  in comparison to the  $\phi'$  the closer the iso- $\alpha$  lines move to the center and the more effective the frontogenetic function. Substituting then the term  $(\cos 2\phi - \cos 2\phi')$  in the last equation we get:

$$(33) \quad F = a(\cos 2\phi - \cos 2\phi')|\nabla\alpha|$$

a most useful equation as it allows the separate consideration of the above mentioned angles.

Summarizing the principles of frontogenesis, it may then be stated that there is a frontogenetic region where the iso- $\alpha$  lines make an angle  $\phi$  with the deformation axis in a deformation field smaller than the frontogenetical angle  $\phi'$ , and similarly that there

is a frontolytic region where the angle  $\phi$  is larger than the  $\phi'$ . This is shown for a simple case in Fig. 18.

The value of  $F$  is the product of  $\cos 2\phi - \cos 2\phi'$  multiplied by the scalar value of  $|\nabla\alpha|$ . Naturally the distribution of  $F$  is in coincidence with the distribution of  $|\nabla\alpha|$  provided that the iso- $\alpha$  lines are nearly parallel to each other. A study of the streamlines shows that the line of frontogenesis moves with the current of the field but that it remains a substantial line which will in time be intensified into a real front or will change a weak front into a strong one

Fig. 18

Fig. 19

Under the frontogenetic conditions the process of frontogenesis can be illustrated by the above diagram, Fig. 19. Since the iso- $\alpha$  lines are in a field of motion the particles will be carried along the stream lines.  $\phi$  in this case has been chosen less than  $45^\circ$  with the X-axis and  $b$  has been neglected, in which case the iso- $\alpha$  lines as shown are brought closer together after a time  $t$ . The solid iso- $\alpha$  lines represent the original configuration and the dotted lines the changed configuration of the iso- $\alpha$  line field after a time  $t$ .

Examining the diagram we can find that there are two kinds of motion which have affected the changes in the iso- $\alpha$  line field, namely, the rotation of the lines towards the X-axis and the moving of the iso- $\alpha$  lines towards each other. These correspond to the two terms in the equation of F. The rotating motion will not stop until the iso- $\alpha$  lines are parallel with the X-axis but it can be stated that the frontogenetic function will only be positive when  $\phi$  is less than  $45^\circ$  with the X-axis (in the above general case). For when  $\phi$  is greater than  $45^\circ$  originally, the stream lines of the field of motion have to rotate the iso- $\alpha$  lines for just so much longer a period before frontogenesis can become effective. The time needed for this pre-FG work together with that necessary for FG may often be of such duration that the pseudo-conservatism of the air mass properties is overcome so that in regions with the iso- $\alpha$  lines originally oriented at angles of more than  $45^\circ$  with the X-axis, conditions are unfavorable for FG and the greater the angle the less favorable, as may be shown in computation of the magnitude of the frontogenetical function under varying conditions.

IV.

SOURCES AND TREATMENT OF MATERIALS

The concepts presented above form the basis for the treatment of the Frontogenetic regions of the Far East. Presented herewith, data at the present time is insufficient for an exact study of all phases of the subject in these regions.

There is available only surface wind data, a few iso-thermal charts and the daily weather maps from various sources. The principal material for the study of the fields of motion in the Far East were found in the papers written by W. Werenskiold (5) and C.C. Chu(6). W. Werenskiold integrated the mean air transport over the North Pacific Ocean into resultant streamline pictures for the various months, while C.C. Chu has listed the mean monthly wind force and the prevailing wind directions in January, April, July, and September for eighty stations in China. Combining the two sets of data a rather complete chart of atmospheric circulations covering the North Pacific Ocean, the Japanese Islands and the coastal regions of China can be obtained for each season of the year.

These seasonal wind charts form the principal aid in finding the deformation fields in the Far East. It is rather regrettable that the data are restricted to water regions and sea coasts but in the same light because of the smoothness of the surfaces over which the air moves, the flow should be representative.

The only air mass property available was surface temperature, obtained from scattered sources: namely (7) a paper by C.C. Chu, "The Thermometric Charts of the Zi-Ka-Wei Observatory (8), the Pilot Charts of the North Pacific prepared by the U.S.N.

Hydrographic Office (9) and the daily weather maps of the Zi-Ka-Wei Observatory and the Imperial Marine Observatory, Kobe, Japan. The temperatures given in C.C. Chu's paper have been reduced to sea level while the data over the ocean on the Pilot Charts are naturally at sea level. It is an advantage that these latter data should be intrinsically representative. The daily temperature reports given on the weather charts should also be of similar character since most of the stations are in sea level regions. Change of pressure will only vary the temperature about 2 to 3°C. so the isotherms may be considered as approximate potential temperatures. Daily inland temperatures would not be representative but by using the mean of long term records this error is negligible.

The procedure in the treatment of these data is as follows: First from a given wind chart a deformation field is located and the values of the coefficients a, b, c, determined. Next from a superimposed isotherm map the distribution of  $|\nabla\alpha|$  is found. From these calculations and measurements the value of F at various points can be found and from the field of F the line of Frontogenesis can be located.

A deformation field can be easily found when a streamline picture of the atmospheric circulation is obtained from a careful study of wind charts and a precise construction of the streamlines. The values of a, b, and c, are obtained by using the equations previously introduced, ie.:

$$\begin{aligned} u &= u_0 + (b+d)x - cy \\ v &= v_0 + cx + (b-d)y \end{aligned}$$

Since a center is defined as a point where u and v vanish simultaneously, for a center at  $X_0, Y_0$ , we have:

and 
$$X_0 = \begin{vmatrix} -u_0, -c \\ -v_0, b-d \\ b+d, -c \\ c, b-d \end{vmatrix}$$

$$Y_0 = \begin{vmatrix} d+b, -u_0 \\ c, -v_0 \\ d+b, -c \\ c, b-d \end{vmatrix}$$

If  $b^2 - a^2 + c^2 \leq 0$  the field will have a center. By parallel translation of the system of coordinates to the center we obtain

(dropping indices):

$$\begin{aligned} u &= (b+a)x - cy \\ v &= cx + (b-a)y \end{aligned}$$

Substituting the above in the equation of a straight stream line thru the center we get:

$$\frac{dy}{dx} = \frac{y}{x} = \frac{v}{u} = \frac{a \pm \sqrt{a^2 - c^2}}{c}$$

In this last equation the actual value of the slope of a straight streamline through the center relative to the X-axis can be readily obtained from a given deformation field graphically and therefore the values of a in terms of c found for that line. For a curved streamline the equation is:

$$\frac{dy}{dx} = \frac{v}{u} = \frac{cx + (b-a)y}{(b+a)x - cy} = \frac{c + (b-a)\frac{y}{x}}{b+a - c\frac{y}{x}}$$

For determining b in terms of c, the above equation is used.

Taking a system of coordinates thru the center of the deformation field shown above the slope  $\frac{y}{x}$  is constant along any straight line thru the center and can be found for points in any deformation field. The values of  $\frac{v}{u}$  for these same points are similarly obtained from the curved streamlines through the points. In order to make the value of  $\frac{v}{u}$  more representative, in actual practice measurements were made at many points <sup>along</sup> a straight line drawn thru the center and the mean value taken. With this value of b obtained from the curved streamlines and the value of a previously found from the straight streamlines the ratio of b/a for a given point is calculated. From this the width



of the frontogenetic sector may be readily computed from eq (32). This together with the values of a,b and c, found for the deformation field chosen are shown on the accompanying charts, along with the small sketch in the corner which shows the direction of the deformation axis.

For the second part of the formula, the relative value of  $|\nabla\alpha|$  is measured from the isothermal chart where the isotherms are taken as the iso- $\alpha$  lines, according to the formula  $|\nabla\alpha| = \frac{1}{h}$ , h being the normal distance between two adjacent lines. All the contour lines of  $|\nabla\alpha|$  are the result of measurement of  $|\nabla\alpha|$  through the field.

After the  $|\nabla\alpha|$  chart is prepared the F for a given point is obtained by multiplying the value of  $|\nabla\alpha|$  with the  $\cos 2\phi - \cos 2\phi'$  term. This latter term includes the measurement of  $\phi$  taken through the whole field. Repeating these extensive calculations contour lines of F can be drawn. Finally through the points of of maximum curvature of these F contours a line can be drawn which represents where the frontogenetic function is most effective. If any new front is to be formed or an existing front is to be intensified it can be expected in this region.

V.

AIR MASSES AND FIELDS OF MOTION IN THE FAR EAST.

(10)

In a previous paper the author has made an investigation of the air masses of North China. The Air Masses classified therein are the Polar Siberian ( $P_S$ ), the Tropical Pacific ( $T_p$ ) and the Polar Pacific ( $P_p$ ) types. They are found to be the principal types in the Far East and play the important roles in Frontogenesis in that region.

However, one additional type of Air Mass, the Equatorial Pacific ( $E_p$ ), which may be distinguished from the general type of warm  $T_p$  mentioned above is considered here. There are several definite reasons for considering this distinction. First, the stream lines over the tropical region of the North Pacific Ocean clearly show a discontinuity between the air coming from the semi-permanent Pacific High and that from more southerly regions. This discontinuity line is called by W. Wernskiold the "equatorial line of convergence" in his work and is probably coincident with the "Intertropikfront" mentioned in 'Physikalische Hydrodynamik' by V. Bjerknes. This line can even be verified by a wind shift on the daily weather charts of the Far East, in the summer season. Secondly, the different identity of the air masses is shown by a comparison of the soundings in  $T_p$  air made at Honolulu, Hawaii, which is in the  $T_p$  belt and those made in  $T_p$  air on the China coast which comes from a more southern region of the Pacific Ocean. This fact has already been pointed out and discussed by the author in his paper "Air Masses of North China".

Therefore it is logical to subdivide the general type of  $T_p$  mass into two sub-types of warm, moist air. The one which is

on the north side of this discontinuity line will still bear the original symbol  $T_p$  denoting the air mass as originating in the sub-tropical zone of the North Pacific Ocean. The other which comes from the more southerly regions of the Pacific Ocean will be identified by the new symbol  $E_p$ . The line of discontinuity or "equatorial line of convergence" will thus mark the boundary of the two air masses.

This Equatorial Pacific air mass comes to the region of the Far East only in the summer season. Beginning in the late Spring season a low pressure area gradually forms in the northern part of Indo-China. As the thermal equator which is the hottest belt on the globe continues to move northward after the sun, the low pressure area is enlarged and becomes almost a permanent system on the daily weather charts of the Far East during the months June, July, and August. This low pressure system undoubtedly induces the  $E_p$  air to come from the south across the geographical equator, appearing as a steady south to southwest wind due to the influence of the earth's rotation. E. Gherzi<sup>(13)</sup> called this current the Philippine Stream coincident with the path it frequently takes. It is not clearly known to what limits the current extends into Asia, (a rough idea can be found in the author's previously mentioned paper under the section devoted to  $T_p$  air masses and also in C. C. Chu's paper "Circulation of atmosphere over China" under the section on wind direction in July), but its activity around the Philippine Islands, the southern China coast and the adjacent seas during the summer is well known.

The Polar Siberian and the Tropical Pacific however remain the

two principal Air Masses in the Far East. They appear almost all the year and continuously converge over the region to form a marked frontal zone. However, this zone is an oscillating one due to the normal monsoon tendencies of the region. In the colder half of the year the frontal zone will lie at some distance offshore and in the warmer part of the year near the coast or inland. In the spring and autumn the P<sub>s</sub> mass easily develops into a certain type of modified air found to exist in the zone between the two principal types. This modified type of P<sub>s</sub> warrants consideration as it still has frontal importance in the Far East as will later be shown.

Due to the essential difference of their source regions, the P<sub>s</sub> and the T<sub>p</sub> air are quite different in their properties. From the sounding data obtained in China the average value of  $\theta_E$ , the equivalent potential temperature, for P<sub>s</sub> air is around 270-280°A. in the winter season, 290-300°A. in the Spring and Autumn and 310-320°A. in the summer. The properties of T<sub>p</sub> air are not clearly known in Asia due to a lack of sounding data, however they can be judged by data obtained in other locations. The  $\theta_E$  value of T<sub>G</sub> and T<sub>A</sub> in the U.S., which have a similar circulation to the T<sub>p</sub> air in Asia, is about 320°A (14) during the winter season. At Honolulu, at a lower latitude the T<sub>p</sub> air has a winter value of about 340°A. Using the mean value of the above two sets of data to give a rough idea of the value of T<sub>p</sub> air in Asia and comparing it with the winter value of P<sub>s</sub> air, we can conclude that there is a temperature difference of 30-40° between the two principal types, P<sub>s</sub> and T<sub>p</sub>. This

throws some light on the resultant frontal and cyclonic activity to be expected between the two masses.

The fourth air mass  $P_p$  is the least known on the China coast and is likewise of least importance in considering Frontogenesis in the Far East. However there must be a fairly large temperature difference between the  $T_p$  and  $P_p$  air because of their different origin and becomes most effective in producing fronts where they meet over the Northern part of the North Pacific Ocean throughout most of the year. The resultant interaction between them might well be the cause of the intensification of an existing front or of a cyclone as it moved up from the south.

#### Fields of Motion

The field of motion of the atmosphere in the Far East is distinctly controlled by two well known semi permanent anticyclones the Pacific High in the southeast over the ocean and the Siberian High in the northwest over the land, together with the well known cyclonic system 'the Aleutian Low' in the northeast as the focal center of their outflow. The Pacific High has a permanent seat in the 'Horse Latitude' Zone between longitude 140 to 150° W. It shrinks and enlarges its dominating area in the course of the year, but it exists at all times. The most active period is the summer when the ocean temperature is lower than the temperature at the same latitude in adjoining land areas.

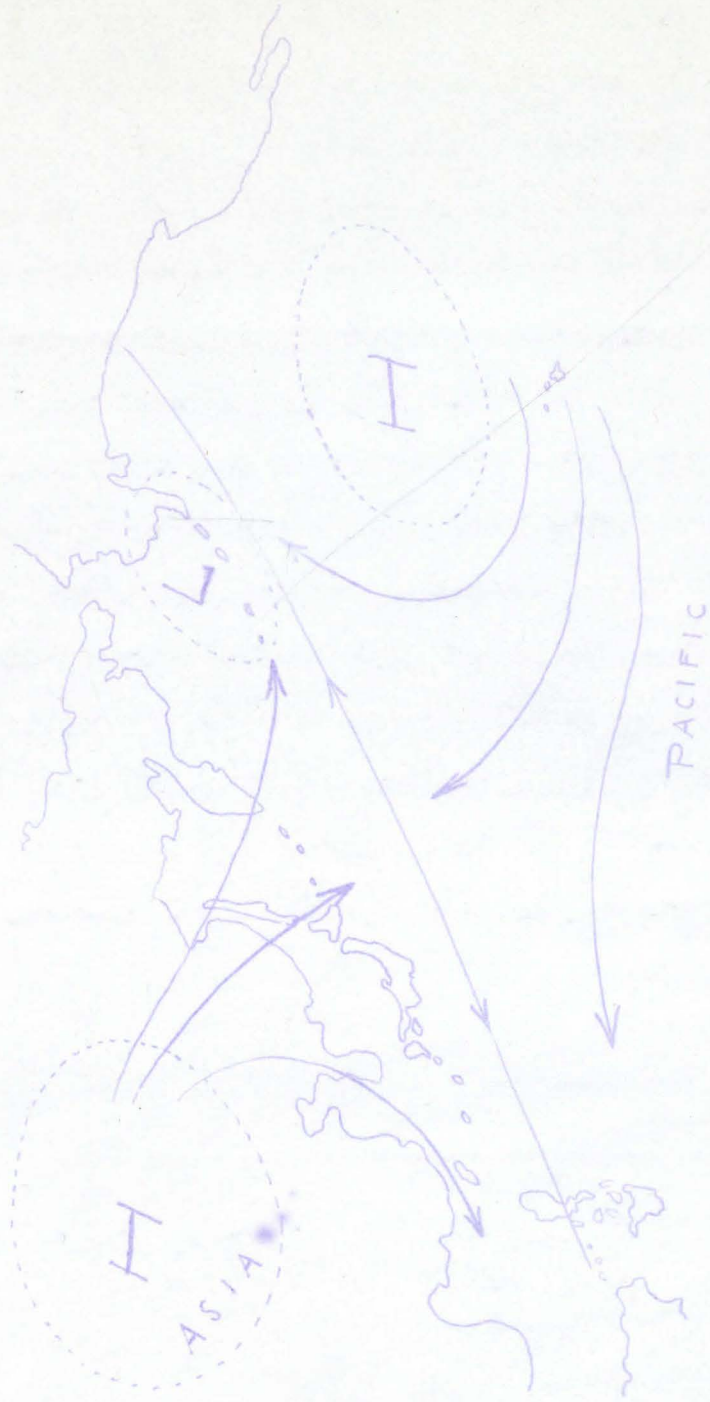
With a more intensive center than the Pacific High, the Siberian High on the continent is most active in the winter season.

During the summer it almost disappears as it retreats poleward. However the low center for Asia land areas in summer is still far to the southwest of India and Persia (based upon the map of pressure distribution in "Physikalische Hydrodynamik" which (15) indicates that the air flow still comes from Siberia at this time. (16) C.C. Chu has mentioned the northerly winds in Sinkiang, West China, during the summer season, which would verify the existence of a northern current in the inland of Asia during that season. Occasionally a High in Siberia or northwest China can be found on the weather charts of the Far East during the mid-summer period also. Therefore the continuance of this frontal zone can be expected during the summer even though the  $P_s$  source is not as easily seen as in the winter.

The Aleutian Low in the northeast is likewise semi-permanent in its nature. Of course, it is more pronounced in the winter than at any other time because the region is comparatively warmer than the continents on the two sides of the low at this season.

From these semi-permanent pressure systems we can expect a field of motion of the deformative type for the Far East as a whole, as shown below (Fig. 20). The dilatation axis of the deformation field runs in a southwest-northeast direction roughly paralleling the coast. Since this particular distribution of pressure in the Far East is not entirely up-set in any season of the year, the field of motion is nearly a standard one for the region. It should be best developed in the winter season, however, because both the cyclone and anticyclones controlling it are

FIG. 20. THE GENERAL FIELD OF MOTION IN THE FAR EAST



well defined in their location at this season. For other seasons though modification has occurred to a considerable extent the essential shape of the field of motion is still about the same and the orientation of the deformation axis remains about fixed. P. Bergeron, based his statement upon this consideration in pointing out that the Far East is a region of Frontogenesis. (17)

However the field of property (isotherms) must also be studied in its relation to the field of flow because  $F$ , the frontogenetic function as shown above is a function of  $\phi$ , the angle between the isotherms and the deformation axis and the magnitude of the temperature ascendent. If the isotherms in the Far East should make a very large angle, say larger than  $\phi'$ , (the angle of the frontogenetic sector) with the deformation axis then there would be frontolysis instead of frontogenesis. This is the point which has to be determined in practice and which will be treated in the examples to follow.



VI.

FRONTOGENETIC REGIONS IN THE SPRING SEASON

Theoretically it is not possible to apply the principles of frontogenesis in a linear field of motion, as discussed above, to a study of frontogenesis in a large field of motion between two air masses from different source regions because in such a large field the motion will no longer be linear. Thus in this study we shall restrict the area of investigation to a vicinity where frontogenesis is expected. In this way the field under consideration will be small and the general theory of frontogenesis in a linear field of motion can still be used.

The effect of the various seasons of the year on the set-up of the various fields will first be considered. Spring is the season when the Siberian High on the land begins to weaken though still active while the Pacific High on the ocean becomes more pronounced. As the Siberian High becomes weaker and more elongated, it has a tendency to split up and a secondary High form over the Japanese Islands. This High forms a modified  $P_g$  air mass over the ocean. Thus the resultant field of motion in the Far East is a little more complicated by this addition than at any other season. The fields will exist between these Highs and the Aleutian Low to the northeast.

From the wind chart over the North Pacific, we find three well defined deformation fields as a result of the above distribution of pressure. One, labelled Deformation Field 2, is over Japan

proper, and a third, Deformation Field 4, is far to the northeast in the vicinity of the Aleutian Islands, (Chart 1). Continued study of a combined wind chart showing ocean and continent data indicate the presence of another field. On the land wind directions along the China Coast clearly show a line of convergence between the on-shore and the off-shore currents. It is evident that there is a line dividing the different wind directions in the on shore current at a point somewhere near the outlet of the Yantze River. Winds south of this line are generally northeast, while north of it they are southwest, (Chart 2). This line is apparently the axis of contraction of a deformation field. Other branches of the circulation substantiate the existence of this, Deformation Field 3, along the coastal provinces of China.

Of the above four deformation fields, number 1 is formed by a northwestern current on one side and a southeastern current on the other side. The former current should be modified  $P_g$  air at this season with a rather long life history over the sea, while the southeastern current is naturally  $T_p$ . The resultant field is almost purely deformative in character with the deformation axis running in a southwest-northeast direction. Of the constants in equation (32) coefficient 'b' for this field of motion is equal to zero. Therefore  $\phi'$  is  $45^\circ$ .

Deformation Field 2 is interposed between the modified returning  $P_g$  air on the east side and an opposite current of modified  $P_g$  on the west side which has a shorter life history over water. The field has been rotated a little, but 'b' is

still nearly equal to zero.

Of these two fields, the latter is relatively unimportant since it exists between two modified types of the same air mass,  $P_S$ . On the other hand the properties of the  $T_p$  and the modified  $P_S$  air differ widely and the resultant action in field number 1 will be of major importance.

Deformation Field #3 is, generally speaking, also in one air mass, with fresh  $P_S$  air on the northwest side and modified  $P_S$  air on the southeast side. Since cold and dry  $P_S$  air very easily loses its characteristic properties in moving southward and acquires others by passing over a warm water surface, the properties of these two masses are quite different. Accordingly from a frontogenetical standpoint this field will be more important than field 2. Unfortunately the streamlines over the northwestern sector of the field can not be completely drawn because of insufficient wind data over the region. However the deformation axis indicated by the remainder of the data still seems to be in the northeast-southwest direction. A slight positive rotation is also observed in this field in the northeast.

Deformation field 4 is composed of a current from the southwest and another from the north through the Bering Strait. The two currents involved, due to the high latitude of the place would be Polar Pacific and Polar Arctic air respectively. Because of its location outside the region of the Far East it has not been investigated in this paper.

Although three well defined deformation fields are found in

the Far East, it is discovered upon studying the isothermal field superimposed on the field of motion that only two fields will have frontogenetical importance. D.F. 2 is not only insignificant for frontogenesis from the standpoint of the air masses involved as has already been pointed out, but also when the orientation of the isotherms in the field of motion is considered, since they make an angle larger than  $\phi'$ , in this particular case larger than  $45^\circ$ , with the deformation axis. The value of  $F$  cannot therefore be positive, until an appreciable rotation of the isotherms in the field of motion has been accomplished.

In D.F. 1 however the angle  $\phi$  is everywhere smaller than  $\phi'$ . The Frontogenetical function  $F$  is positive throughout the field and a line of frontogenesis is obtained along the east coast of Japan parallel to the deformation axis of the field. (Chart 3&4) The parallel direction of these two lines results from the orientation of the isotherms nearly parallel to the deformation axis of the field.

D.F. 3 has an angle  $\phi$  smaller than  $\phi'$  in some parts of the field, particularly in the northwestern half, but larger than  $\phi'$  in the remainder of the field. This together with the large value of  $|\nabla\alpha|$  in this region yields a large positive value of  $F$  in the northwestern portion of the field, which locates the frontogenetic line far inland. It should be noted again that the streamlines in the northwest section of the field are not completely drawn and similarly the isotherms are possibly doubtful due to the insufficiency of the information pertaining thereto. The line of fronto-

genesis determined for this field may then vary somewhat from its indicated position, particularly as the deformation field changes.

The above two lines of frontogenesis determined for the region of the Far East during the Spring season denote places where frontal systems are likely to be developed or intensified. The one determined from D.P. 1 is the main frontogenetic line in the Far East. The air masses involved are essentially different and in this season produce the most intense systems in the region. The other line is a secondary line of frontogenesis because it is still within one general type of air mass, namely Ps. Therefore with an even chance for frontal action the development of the latter front will not be as intense as the first. An examination of the daily weather charts for the Far East indicates a correspondence between the frontogenetic lines mentioned above and the cyclonic tracks. Since the latter can be regarded as the traces of disturbances moving along a front the verification is excellent. Published herewith is a chart (Chart 5) of cyclonic tracks in the Far East for the month of April reproduced from the daily weather charts of the Imperial Marine Observatory, Kobe, Japan. It is rather interesting to note the two general groups of cyclonic tracks that seem to correspond very well to the two lines of frontogenesis. Another paper, Shio-Wang Sung's Chart of the Normal Tracks of Extra Tropical Cyclones of Eastern Asia also shows this agreement.

The tracks in the southern group are so identical with the

main frontogenetic line that their location and direction are apparently the same. Worth noting is the fact that the cyclones following these tracks in the southern group are usually strong, which is to be expected from the strong interaction between the  $T_p$  air and the modified  $P_g$  air along the main frontogenetic line.

What is of greatest interest from the standpoint of this investigation, however, is that in April there is no cyclonic track passing through North China according to the Japanese Marine Observatory's Chart. A reference to the reproduction made here of Shio-Wang Sung's series of Normal Tracks, shows his Number 3 track suddenly changing in direction from the east down to the south at a point near latitude  $47^\circ$  and longitude  $115^\circ$ , leaving a wide area of North China free from cyclonic activity. Actually during this period North China always suffers from dry weather and in serious cases even drought may result from this cyclonic and frontal inactivity.

The reason for this inactivity is not due to the air mass itself because there exists a prevalent onshore current of modified  $P_g$  <sup>(19)</sup> during April. The fundamental reason is shown by a glance at the chart of 'F' for April. The negative value of F in the region of North China results from the large angle  $\phi$ , between the isothermal lines and the deformation axis there.

The secondary line of frontogenesis in the Far East appears among the northern group of cyclonic tracks, as determined from the sources mentioned above. The direction of the line closely parallels the cyclonic tracks reproduced from the Japanese weather charts. This close relation indicates that the line is apparently responsible for the observed development of these frontal cyclones.

VII.

FRONTOGENETIC REGIONS IN THE SUMMER SEASON

The summer wind condition in the Far East is entirely controlled by the Pacific High. The High in this season has moved from its winter position of around  $34^{\circ}$ N. and  $140^{\circ}$  W. Longitude to a center at about  $42^{\circ}$ N. and  $150^{\circ}$  W. At the same time the pressure increases from the winter average of 1020mb. to (20) a seasonal value of 1025mb. while its area increases significantly with its 1015mb. isobar extending northwestward about  $20^{\circ}$  into a position near the Japanese Archipelago.

On the other hand over the land, the Siberian High at this time appears to exist only in the western part of Siberia. The result of this pressure field readjustment gives a steady pressure gradient from ocean onto the land. A southeast to southwest warm marine current covers the entire region of the Far East being popularly called the 'Summer Monsoon' of Asia.

From the available wind data in the Far East one main deformation field can be found for this season. The field is formed by the above mentioned 'summer monsoon' from the south and the northern polar current from Siberia. There are several indications to verify the existence of this northern polar current in northwest China during the summer season, although as mentioned above, the Siberian High is not prominent on the map. At two stations, Tiwha or Urumchi (Lat.  $43^{\circ} 45'$ N., Long.  $87^{\circ} 40'$ E.) and Kuchar (Lat.  $41^{\circ} 40'$  N., Long.  $83^{\circ} 00'$ E.) in Sinkiang Province or Chinese Turkistan and one station, Chunching (Lat.  $29^{\circ} 33'$ N., Long.  $106^{\circ} 33'$ E.), in the Szechuan

Province, western China reported prevalent north and northwest winds in July, while prevalent wind directions at all the eighty stations scattered along the China Coast and Coast Provinces are southeast to southwest. C.C. Chu noting this says that the summer monsoon "seems to have reached its northern limit" in southern Mongolia. <sup>(21)</sup> Probably a logical position for the boundary of the summer monsoon and the northern polar current in the summer will be, just through Hutjertugol to Chun-ching in a northeast-southwest direction.

(22)

V. Bjerknes and others in their book show the center of the summer deformation field in Asia to be in a place somewhere near North Manchuria, during the month of August. From the author's determination, the center in July seems to be in the northwestern corner of Inner Mongolia. This can be verified by drawing a line dividing the winds in the summer monsoon, from the northwest winds to the North which line seems to be the axis of dilatation of the deformation field. The line runs in a SW-NE direction across North China and Manchuria. If we allow this line to be the dilatation axis of the deformation field the center of the field will be along the line at its intersection with the contraction axis which is readily located in the divergent field of the monsoon winds. This center appears to occur in the southwest corner of Inner Mongolia. Generally speaking, this deformation field is in good agreement with that drawn by V. Bjerknes and his co-authors for the period one month later. The dotted stream lines in the northern current indicate that they are a little doubtful due to a lack of data.



A glance at the July Deformation Field Chart (Chart 6) shows that the main field on the Asia continent is a pure deformative type with the deformation axis which in this case is the dilatation axis running in a SW-NE direction. Since the isotherms in the field are quite irregular the distribution of  $F$  is not coincident with the contour lines of  $|\nabla\alpha|$  as is usually expected. Over the Japan sea the isotherms show a trough as the effect of the well known Okhotsk sea Current, coming down from the Okhotsk Sea in the north, and cooling the air at the surface over this region. Along the southeast border of Inner Mongolia the isotherms show another trough. The wedge shaped isotherm field between these two troughs apparently indicates the domination of this territory by the warm maritime air of the summer monsoon from the south. This again shows that the line of convergence between the summer monsoon and the northern polar current must exist there as indicated by the dilatation axis of the field.

The frontogenetic line of the field, due to this particular feature of the isotherm field, should only extend from Whang Ho or the Yellow River valley to Manchuria running in the SW-NE direction along the deformation axis of the field. (Chart 7&8). This line is the main frontogenetic line for the summer season in the Far East because as seen from this analysis it is derived from the main deformation field formed by the two principal types of tropical maritime and polar continental air masses.

A comparison between this frontogenetic line and Sung's normal cyclonic tracks in the Far East (Chart 9) show the line in good

agreement with track No. 1 and track No. 2. which are the tracks of about 70% of the cyclones in the summer season. On the Japanese Weather Charts the actual cyclonic tracks in July, 1933 do not follow the frontogenetic line very well, but generally speaking their origin is concentrated around this line.

One significant point concerning this field and its location is that both the Japanese Charts and Sung's cyclonic track Chart for the summer season show no cyclone tracks passing through the region between the Whang Ho and the Yantze Valley where a region of frontolysis exists. This is indicated on the Chart of Distribution of  $F$  in the Far East for the month of July. (Chart 8)

Besides the main deformation field for the season a field of special interest is found in the southwest corner of the North Pacific Ocean. This field is identified according to stream line patterns as a curved streamline field without center. (see stream line pattern chart, Fig. 16). The Air Masses involved in this field are the Equatorial Pacific on the southwest side and the Tropical Pacific on the northeast side. The convergence of the air flow which is called by W. Werenkiold the "equatorial line of convergence" and in Bjerknes' book the "Intertropikfront", is a curved line running in a SE-NW direction. Along the line convergence is appreciable. Since the properties of the  $E_p$  and  $T_p$  air masses are not essentially different as observed at the surface an active frontal system could not be expected but nevertheless the formation of the Typhoon in the Far East can be explained by the existence of this special field. The Typhoon is a tropical cyclone

of unusual violence formed on the edge of the doldrum belt. The vigorous nature of these tropical cyclones is undoubtedly due to the large amount of energy available in the two adjacent warm maritime air masses  $E_p$  and  $T_p$ , each with high temperature and humidity.

What we need here to explain the formation of the Typhoon is the introduction of rotation to start the vortex motion, since their origin seems to be in this zone between these two types of air. Petterssen, from a hydrodynamic equation  $\dot{v} = -S \nabla P - \lambda \times v$

where  $S$  is the Specific Volume,  $P$  the atmospheric pressure,

$\lambda$  a vertical vector whose magnitude is  $2\omega \sin \phi$ ,

$\omega$  being the velocity of earth's rotation,  $\phi$  the latitude and  $v$  a vector representing velocity, has pointed out that convergence produces positive curl or cyclonic rotation as shown by the following equation:-

$$\frac{d}{dt}(\text{curl } v) = -\text{div. } v(\lambda + \text{curl } v) + \nabla S \times (-\nabla P)$$

where the last term  $\nabla S \times (-\nabla P)$  is the number of solenoids in the horizontal plane and is usually quite small, especially in the Typhoon region where the temperature distribution is practically uniform. Having neglected the last term, the equation is

$$\frac{d}{dt}(\text{curl } v) = -\text{div. } v(\lambda + \text{curl } v)$$

expressing the rate of change of curl  $v$  with time as proportional to the convergence of  $v$  ( $-\text{div. } v$ ) times the bracketed term. From this equation we can further solve curl  $v$  to obtain a more detailed expression for the relation between curl  $v$  and  $-\text{div. } v$ .

Let the two vectors be expressed

$$\text{Curl } v = iX + jY + kZ, \quad \lambda = iA + jB + kC$$

and take the average  $-\text{div}.v = -b$ , then:-

$$\frac{dX}{dt} = -b(A+X) \quad (1)$$

$$\frac{dY}{dt} = -b(B+Y) \quad (2)$$

$$\frac{dZ}{dt} = -b(C+Z) \quad (3)$$

Rewriting equation (1) :  $\frac{dX}{dt} + bX = -bA$  (4)

and taking the integral we have:  $X = e^{-bt} \left( \int -bAe^{bt} dt + K \right)$  (5)

$$= e^{-bt} (-Ae^{bt} + K) \quad (6)$$

$$= -A + Ke^{-bt} \quad (7)$$

At  $t=0$ , and  $X = 0$ ;

$$0 = -A - K, \text{ or } K = A.$$

Equation (7) then becomes  $X = A(e^{-bt} - 1)$  (8)

similarly  $Y = B(e^{-bt} - 1)$  (9)

$$Z = C(e^{-bt} - 1) \quad (10)$$

therefore  $\text{Curl } v = \lambda(e^{-bt} - 1)$  (11)

Equation (11) indicates that curl  $v$  is a function of  $\lambda$  and increases exponentially with the increase of convergence, i.e.  $-\text{div}.v$ , and time  $t$ . In the field of motion referred to above convergence is quite pronounced so that a positive curl  $v$  is very easily produced and intensified. However, near the equator, where the latitude angle  $\phi$  is small and  $\lambda$  is small, curl  $v$  still has a small value. With the increased value of  $\lambda$  with the increase of latitude curl  $v$  must become active even with the magnitude of the convergence ( $-\text{div}.v$ ) remaining the same. This explains why Typhoons are usually formed along the line of convergence between  $E_p$  and  $T_p$  at latitudes not lower than  $10^\circ$  and are quickly intensified as they move to higher latitudes.

From the above discussion of the formation of Typhoons the movement of these storms can further be analysed. In the tropical zone the Typhoon should follow a path where the convergent flow is most active in order to maintain and intensify its vortex motion. Therefore the "equatorial line of convergence" is naturally the normal track of the Typhoon as will be borne out by later investigations.

Upon the arrival in the temperate zone, however, the "equatorial line of convergence" is no longer distinct, but the temperature variation begins to play an important part. In other words as the storm begins to assume the position of an Extra-tropical Cyclone it will be influenced by frontogenesis at this latitude. During the summer season there is a region of frontolysis along the China coast and over the coastal provinces, while a slightly frontogenetic region exists to the east over the ocean. This distribution of the frontogenetical functions will give a degenerating effect to the typhoon as it moves inland but will help to regenerate it as it moves over the ocean.

The primary factor governing the movement of the typhoon is the general wind system which has a deep southwestern current over this region. Therefore it appears natural that the typhoon reaching these latitudes recurve northeast whereupon the frontogenetic effect of the ocean maintains the storm's intensity. If the field of motion deflects the storm on land, as is rarely observed in these latitudes, the frontolytic effect thereon helps to destroy it.

The line with the frontogenetic symbol in the southwest corner of Chart VIII, is sketched in accordance with these ideas of typhoon movement. Actually most typhoons in July and August do follow this track into the middle latitudes as observed on Chart IX. Before the month of June and after September the "equatorial line of convergence" based on charts of averages, is no longer observed in the Far East and since the occurrence of a typhoon is generally rare during that period, this seems to give material proof that the formation of the typhoon is definitely related to the convergent flow along the "equatorial line of convergence" between these two air masses,  $E_p$  and  $T_p$ .

The study of actual Typhoon formation in this particular field of curved streamlines without center has enabled the author to find a close relation between the position of the center of the Pacific High and the formation of Typhoons in the Far East. Briefly stated the relations are as follows:- When the Pacific High is displaced to the east from its normal position the low pressure region over the ocean northeast of the Philippine Islands is increased. At this stage southwest winds are active over the South China Sea while light and irregular winds are observed in the flat pressure field northeast of the Philippines. When the Pacific High starts a return to its more average position as shown by a westward extension of the isobars and of the northeast trades, the winds in the flat pressure region mentioned northeast of the Philippines begin to show a cyclonic circulation. This development continues with the southwestward movement of the Pacific High or an intensification of the High Center itself. As the cyclonic center moves into higher latitudes an active Typhoon is formed. Actual examples

can be easily obtained from the summer weather charts. One example is given here in Charts (10) to (13). It is seen that during the four days of formation of the resultant Typhoon the Pacific High has moved a long distance from northeast to southwest. At the same time the westward movement of the 'Equatorial line of convergence' as shown by a zig-zag line on the map can also be traced.

Conversely it is important to note that Typhoons are rarely observed in the Far East when either, the Pacific High is moving towards the east, or it remains in the east, or it already occupies an extreme western position at the same time that the center is well developed.

The correlation of the facts above noted in the formation of Typhoons can be explained by the theory of Typhoon formation based on the convergent flow occurring in the curved streamline field existing in the southwest corner of the North Pacific Ocean. The first essential appears to be the movement of the Pacific High which decreases the pressure gradient over the region normally occupied by this line. This allows a flow of  $E_p$  air from the southwest into the region to be established. Next when the Pacific High moves back from the east it naturally increases the pressure gradient towards the southwest and extends the northeast current to meet the  $E_p$  current mentioned. This convergence produces cyclonic curl and explains the cyclonic circulation which forms at this time. A continuance of these conditions allows the Typhoon to be developed.

As a check on this it appears that when the Pacific High moves into an extremely western position and remains active the

'Equatorial line of convergence' will be pushed down to a position in the very low latitudes where the term  $\lambda$ , ie.  $2\omega \sin \phi$  is too small to create an appreciable value of curl. Therefore the favorable condition for the formation of Typhoons in the Far East naturally follows the westward extension of the Pacific High after its eastward displacement has allowed an influx of  $E_p$  air with which a convergent flow is established. It is believed that a more detailed study of actual cases occurring in this curved streamline field will establish reliable rules for the forecasting of this phenomena.



VIII.

FRONTOGENETIC REGIONS IN THE AUTUMN SEASON

Generally speaking, the features of the atmospheric circulation in the Far East during the Autumn season can be expected to be quite like those found in the Spring season, because the climatic conditions in the two seasons are essentially similar. However some remarks about the transitional change of the pressure fields can be made here.

The main anticyclone over the Pacific Ocean, the Pacific High, is not as active during the fall as it is in the spring. Not only its dominating area has shrunk but also the center of the High has moved to the north about 6 degrees to a center at about  $38^{\circ}\text{N}$ ,  $142^{\circ}\text{W}$ . On the other hand the main anticyclone on the Asia Continent, the Siberian High, shows an increasing prominence compared to its spring position. The reason for this reversal of activity of the two main anticyclones during the two different seasons can be attributed to the difference in temperatures over the ocean and the land. Due to the high specific heat and mobility of a water surface the ocean temperatures are more reluctant than those over the continent to follow the change of solar intensity during the course of the year. Consequently the continental surface is relatively warm compared to the adjacent ocean surface in the spring season, but colder in the autumn. A glance at the spring and autumn isotherms superimposed on Charts (2) and (14) indicates this difference. These temperature relationships between the ocean and continental areas in Spring and Autumn in a

large measure account for the relative intensities of the principal anticyclones mentioned above.

Under the action of the pressure fields discussed above the deformation fields found for this season in the Far East are basically the same as those found in the Spring, but dissimilar in some points. They total six in number, one in the tropics and five in the temperate zone. (Chart 14) Of the five fields in the temperate zone only one is new while the remaining four can be identified from the Spring deformation field chart. The field not identified from the spring chart seems to be the system located near the Kantchatka Peninsula. This system, however, has no important place in this investigation because of its position outside of the region under consideration. Furthermore the large angle the isotherms in this area make with the deformation axis would only produce frontolysis. Labelling the other four deformation fields in the temperate zone with the same numbers given similar fields on the spring chart the transition of these fields can be examined. It will be noted that Fields No. 2 and 3 show a shift northward and Fields No. 1 and 4 a shift northeastward. Shifting of all of these systems can be directly or indirectly accounted for by the shrinking and northward regression of the Main Pacific High.

The air mass symbols used for the corresponding deformation fields in the spring season can still be used with the one exception of the air mass on the north side of deformation field No. 1 which now may be called  $P_p$  instead of Modified  $P_s$ . This is due

to the northward shift of the minor divergence center (now at  $45^{\circ}\text{N}$  and  $155^{\circ}\text{E}$ ) which will feed air southward from the northern regions of the Pacific Ocean. The symbols are then Tp and Pp for Field No. 1, Modified Ps and either RPs or RPP for Field No. 2, Ps and RPs for Field No. 3 and RPP and AC(Arctic continental for No. 4. <sup>(24)</sup>

The deformation fields themselves are located as before by a careful study of wind data available.

Field No. 3, which is located along the coastal region of the Pei-Chi-Li Gulf is rather difficult to find due to the weak characteristics of the currents in the system. However, on W. Werenkiold's mean air transport chart, there is apparently a divergence center in the Pei-Chi-Li Gulf. Similarly on C.C. Chu's chart of wind data along the North China coast, a line may be drawn dividing the general on-shore current of air along the coast into two groups, with southwest winds on the north side of the line and northeast winds on the south side. Just about 100 miles inland from the Pei-Chi-Li coast to the northwest, a prevalent northwest current is observed. Combining these two currents a deformation field existing over the coastal region becomes apparent. From another standpoint the sudden bending of the isotherms along the coast gives another indication of the presence of this field between two different air masses. Comparing this field No. 3, with its spring counterpart, the activity is decreased because of the diminishing strength of the on-shore current. However, it should be a well defined system retaining frontogenetic importance because of the marked difference between the properties of its Ps fresh from the north and its modi-

fied returning Ps from over the ocean. The position of the isotherms in the field, again limit the frontogenetic action to a small area, but the crowding of these isotherms along the deformation axis is to be noted. Chart (15) of the field prepared for Sept. shows the largest value over the Pei-Chi-Li Gulf and gives the function  $F$  a large value in that region due to the favorable orientation of the isotherms.

Deformation Field No. 1, remains almost the same as in the Spring season. Its characteristics are not changed by the designation of the air on the north side as Pp since the properties of Pp air in that location are about the same as those in the modified Ps air with a long life history over the sea. Therefore the system is just as active and should be the main system of the season in the Far East. Moreover, the action of this field and its counterpart to the NE (Field No. 4) will result in the formation of intense systems passing along their combined dilatation axis. This action is further discussed in a later paragraph.

From the frontogenetic point of view Field No. 2, does not have as important a role as in the spring season, because the isotherms in that field make an even larger angle  $\phi$  with the deformation axis during the autumn than in the Spring due to the added positive rotation of the deformation axis of the system.

The frontogenetic lines calculated from these four principal deformation fields in the temperate zone and the thermal chart for the same season are shown on Chart (16). The southern line is the main frontogenetic line and is coincident with the main

frontogenetic line of the spring season, whereas the northern one over the continental area matches the corresponding secondary line on Chart (4). Between the two lines a region of frontolysis is observed over the Yellow Sea, Korea and the Japan Sea. This frontolytical region is not as large as that noted in the spring season but its location and shape is similar. From this comparison one can readily understand the similarity between the general weather conditions in the Far East in the Spring and in the Autumn.

The relation between the frontogenetic lines and the cyclone movements can be nicely observed on chart (17), where these lines and actual cyclone tracks for the month have been plotted for comparison. It is apparent that the cyclonic tracks have two predominant paths corresponding to the two lines of frontogenesis. On the Japanese Cyclonic Track Chart for September, 1932, there is only one cyclonic track in the northern group while in Sung's normal cyclonic tracks for autumn there are two tracks given with rather definite directions and one with a rather irregular track. The southern group of cyclonic tracks which correspond to the main frontogenetic line both on the Japanese Chart and on Sung's Chart comprise about 70% of the tracks for the season. This preponderance of distribution of cyclones along the southern track as compared with the nearly equal distribution of the two groups in the spring season must be due to the greater activity of the field No. 1 (With its combined action with Field No. 4) over Field No. 3 at this time.

Between the two groups of cyclonic tracks a large area includ-

ing North China and Japan is free from cyclonic tracks as shown on the Japanese Chart and Sung's Chart. This fact is explained by the region of frontolysis on Chart 16 coincident with this area.

An important observation can be made here regarding Chart (17). The cyclone tracks in the southern group show generally parallel directions with the main frontogenetic line for the season, but do not fall along the region of this line. This apparent discrepancy between them can be shown to be due to the fact that the frontogenetic line represents more closely the position of the actual fronts while the cyclonic tracks trace the centers of the cyclone movement only. When a frontal cyclone becomes occluded the center of the system is necessarily removed from the mean position of the front, as shown in the accompanying sketch.

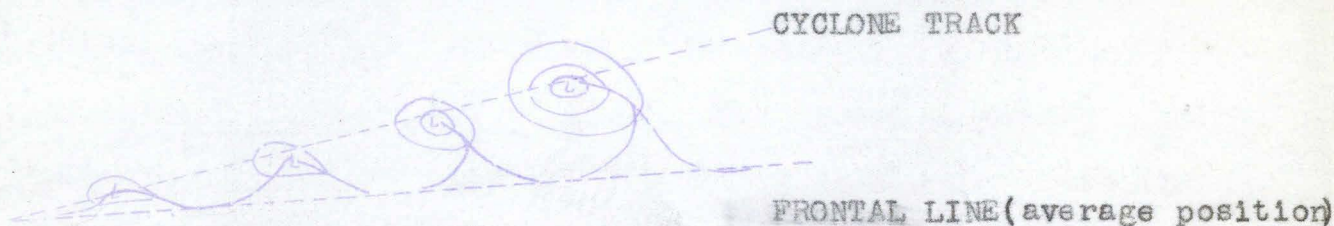


Fig.21

Observing the day to day movement of the center and the main front of the system, two lines can be plotted as shown. It is apparent then that while the center and the front are together at the left of the picture the distance between the two lines will be larger and larger as the system becomes more occluded. This is in agreement with the facts shown on Chart (17) where the cyclonic tracks and the main frontogenetic line are very close to each other

at the southern part of the Japanese Archipelago, but widely separated near the Aleutian Islands.

It is noted that frontal systems along the main frontogenetic line at this season are more active than in the Spring due to the combined action of Deformation Fields 1 and 4 mentioned above. Furthermore the outbreaks of cold air in this season are more intense than in Spring since the Siberian High, which is responsible for the cold air, is more active. These two combine to make the occlusion process more prominent in this season and the separation between the frontogenetic line and the cyclonic tracks should be more noticeable. This is verified by a comparison of Chart (5) for April and Chart (17) for September.

The Deformation Field No. 5, in the southwest corner of Chart (14) in the tropical zone is a remnant of the 'equatorial line of convergence' in the Far East, previously explained in the Summer discussion. It is important only in the formation of the Typhoon. The deformation axis of the system is really the 'equatorial line of convergence' and during this season runs in an almost East-West direction. The interesting thing to note on Chart (17) in connection with this line is that the tracks of two Typhoons occur very close to it. These tracks taken from the Japanese Charts are the only two Typhoons for the month of Sept. 1932. The thumb rule indicating that a Typhoon recurves northeasterly as it moves north is not verified in this case, since these two continued westward along the line of convergence. This seems to further verify the theory that the 'equatorial line of convergence' is the track of Typhoons.

IX.

FRONTOGENETIC REGIONS IN THE WINTER SEASON.

During the winter season the domination of the Siberian High over the Asiatic Continent is absolute. This High is so well defined and so extremely active that its uniform off-shore flow directly reaches the tropical region of the North Pacific Ocean. The Popular name "winter monsoon of Asia" is normally used to designate this flow.

The Pacific High in this season, although not as active as it was in the summer season still is well defined but in a more eastern position and sends a uniform southeasterly flow towards the Far East region. The result is to bring this flow of  $T_p$  into direct contact with the flow from Asia of  $P_s$  air in the winter season.

Inspecting the wind charts of the Far East it is found that one large scale deformation field exists at this time, being well defined in its shape as it is directly <sup>formed</sup> by the two uniform flows coming from the Siberian High and the Pacific High. The field is not a purely deformation type, as the deformation axis of the field is not exactly co-incident with the dilatation axis. A slight convergence is observed in the field, which increases  $\beta'$ , the frontogenetical angle to about  $50^\circ$ .

Another deformation field of much smaller size should exist in South Manchuria because data show a convergent wind flow in this area. This convergent flow consists of a NE to SW current on the east side and a W to NW current on the west side. The small deformation field shown in the northwest corner of Chart (18) represents the plot from the actual wind data available. It is obvious that



in the position shown, frontogenesis cannot be active on the right side of the field because of the large angle, almost  $90^\circ$ , that the isotherms make with the deformation axis, but on the left side frontogenetic possibilities are evident from the decreases value of  $\phi$ .

Furthermore if this field is moved off shore by the strong currents of Fresh Ps, and the counter current of air to the east be maintained, the frontogenetic possibilities become extended through both sides of the field with the new orientation of isotherms offshore. The shape of this particular field shows a pronounced positive rotation, probably due to the influence of the coast line on the orientation of the isotherms. The importance of these factors will be pointed out shortly.

The frontogenetic line for this winter season, as determined from the one large deformation field mentioned above is shown on Chart (20). Thru the field is rather large for considering a linear field of motion in dealing with frontogenesis but nevertheless since the flows in the field are uniform due to each of the Highs being active and the surface traversed by the two flows being smooth, the applicability of the general principles of frontogenesis to this particular case should be much larger than usual. By using the same frontogenetic equation to calculate the value of  $F$ , the line of frontogenesis obtained for winter runs in a nearly parallel direction with the Asiatic coast and not far from it. An examination of this line indicates that its existence in this position results from the large value of  $|\nabla\alpha|$ , or in other words the crowded isotherms along the coastal regions of Asia. (Chart)

The line however occurs within  $P_g$  air. This characteristic makes it different from other frontogenetic lines because it apparently does not represent a region of frontogenesis between two originally different air masses but rather within one air mass. The effect of the small deformation field referred to above now becomes significant, in contributing to the formation of new cold front within the  $P_s$  outbreaks. The counter-current referred to above is evidently maintained by anticyclogenesis behind a cyclone to the east. The formation of such cold fronts between positive isallobaric centers has been pointed out, to the writer, in numerous cases on land by Prof. Krick, and although such detailed data are not available in the observations in this region the action indicates the same result. In addition the positive rotation evident in this field should have an influence in facilitating the formation of wave cyclones on such a front. The important fact that this formation of the new Polar front off the coast of Asia occurs between fresh  $P_g$  air and modified or returning  $P_g$  air has not been previously recognized.

An examination of the cyclone tracks and the distribution of cyclones in this region shows the actual importance of this frontogenetical line. Chart (21) is prepared for this purpose. It can be seen that most of the cyclones during this season occur along this frontogenetic line.

N.V. Stremousov has studied the synoptic processes in the Eastern Part of the Asiatic Continent and the Adjacent Seas. (25)  
The author has not had the opportunity to read his whole paper

but has only had available the English Summaries quoted in the Bulletin of the American Meteorological Society. He points out that 'in winter cyclogenesis shifts from the land to the sea, taking place at the Polar Front between Continental Polar and Maritime Tropical air masses'. The idea that Mr. Stremoussov suggests that winter cyclones in the Far East are formed at the Polar Front is quite true but evidently he felt that once offshore the front occupied a position between Continental-Polar ( $P_s$ ) and maritime-Tropical air masses, ( $T_p$ ). The charts (22-24) here published tend to show that the winter cyclones are formed on the Polar Front before it reaches a position in its southward travel that would indicate the interaction between the  $P_s$  and the  $T_p$ . This can be proved by the fact that most of the winter cyclones in the Far East are started along the southeastern China coast to the Japan Islands where either abstractly considering the position of the Pacific High in the winter season or practically tracing the air flow from the daily weather charts of the Far East, there should be no real maritime-Tropical air. The author has examined many winter charts for the Far East and found that the cyclones are formed at the cold front by wave perturbations during the course of the south eastward movement of the Polar front to its southernmost position between the real maritime-Pacific or  $T_p$  air. This can be theoretically explained by diagram and practically illustrated by examples.

From the theoretical point of view a cold front developing at the frontogenetical line should at first move rapidly southward because of the large offshore pressure gradient always

present along the coastal regions of Asia at this season, as evidenced by the outflow of air from the divergent center of the Siberian High. Under this condition of rapid movement the cold front should be relatively free from wave perturbations and should appear as a smooth curve. As this rapid movement southward begins to diminish the air masses on each side of the front continue to be modified by the journey over the warm ocean surface, and instability develops. Consequently a flat wave is very easily produced along the front and the first step in cyclogenesis is completed.

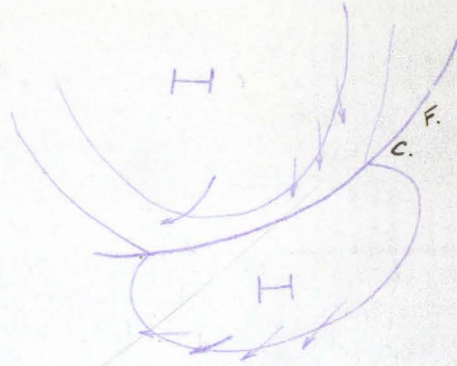
If the main High on the Asiatic Continent still sends a strong current southward the cyclogenesis may remain in this stage, ie. in the form of a flat wave structure, or these waves may even be destroyed. On the other hand the cold front generally becomes less active and the developed wave becomes stronger. Finally an occluding cyclone is formed at the wave crest. An idealized process of this kind is illustrated by the diagrams below: - Fig. 22

As occlusion continues and brings the cold front to its most southerly position where V. Bjerknes and others have shown its average seasonal position to be, it meets the real maritime-Tropical air,  $T_p$ , from the Pacific High, and new waves may tend to develop along it.

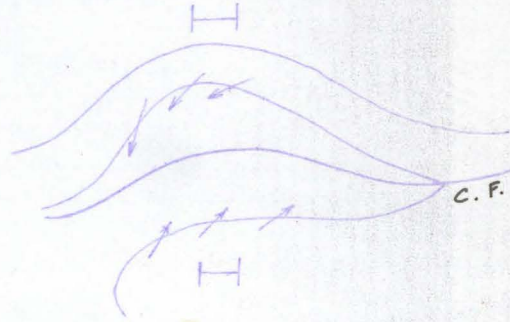
Fig. 22

Ideal case of Cyclogenesis at cold front by a wave perturbation.

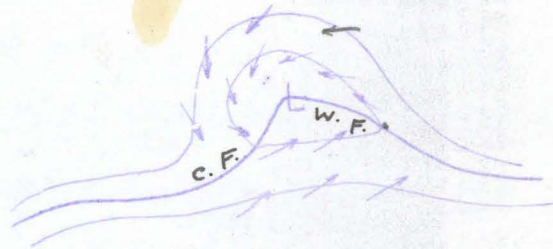
(1)  
Initial cold front



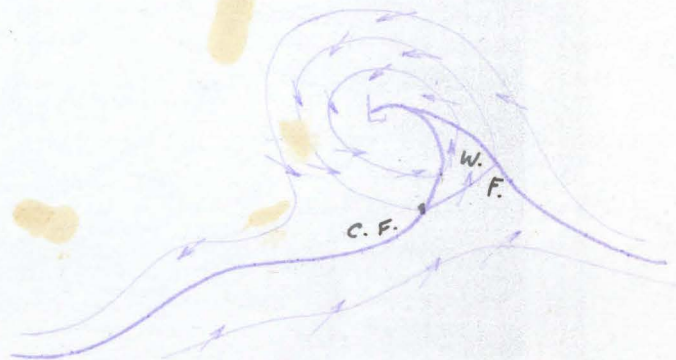
(2)  
First indication of  
Cyclogenesis, the flat  
wave stage.



(3)  
Cyclone stage.



(4)  
Occlusion stage.



Examples of complete and incomplete cyclogenesis from a cold front in the winter season in agreement with the above discussion idea can be easily found on the daily weather charts of the Far East. An example of complete cyclogenesis is given below; (Chart 22-24).

The cyclone chosen for this example only took three days for its full development. The first day, Jan. 15, 1933, of the map series even the front itself which develops the cyclone is hard to recognize. One day later the existence of a frontal system is evident on the map with an apparent wave formation already on the front. Evidently one of the wave crests of the system, probably the foremost one, finally develops into a cyclone near Kyushu Island of Japan as seen on the map for Jan. 17, 1933.

It is clear that there should be no real  $T_p$  air in the warm sector of the cyclone at its inception because the circulation field during these days shows the air with a continuously northerly trajectory behind a previously existing front which has moved southward. Therefore the cyclone is not the result of the interaction between cold Polar Siberian and warm Tropical Pacific air masses but rather between the two types of Polar Siberian air masses previously discussed.

The above example also serves as a good illustration of actual frontogenesis in the field of motion. On Jan. 16, a secondary deformation field is formed in the general frontogenetic region at a position between the China coast and the Japanese Islands, with the resultant splitting of the High in the

north. The deformation axis of this field which is shown on the auxiliary chart for Jan. 16th (Chart 25), makes an angle with the isotherms smaller than the frontogenetic angle,  $\phi'$ , in the region on the west side of this axis. Thus we would expect the development of the frontal system to be accelerated in this territory. Two indications of this development can be observed, first, the increased crowding of the isotherms along the southeastern China coast as shown on the auxiliary chart for Jan. 17th, Chart (26), and by the quickly developed low center on the map for that date. From the deformation field and isotherm chart for Jan. 17th., we can see that the deformation axis of the field has been negatively rotated. The result of this rotation brings the axis and the isotherms more nearly parallel, a condition which would lead to further intensification of the system on the next day. This anticipated deepening is shown on the map for Jan. 18th, (Chart 27) the pressure at the center of the cyclone having dropped from 759mm (29.9in.) to 737mm (29.0) during the 24 hours.

It should be noted that in such cases the cyclone will not develop until some time after the cold front reaches the water, because before that time the front is moving too rapidly and the air is still relatively stable. The fact that most of the cyclones in the Far East during the winter season actually start in the area from the southeastern China coast to the southern part of the Japan Islands already offers proof of this.

(28)

Mr. Richardson, from a statistical study on the distribution of cyclones over the North Pacific Ocean in the winter season, (see Chart 21.), shows that the region of maximum cyclonic frequency is quite far removed from the Pacific Polar Front (Pazifische Polar front of Paz.PF) as determined by V. Bjerknes and others in their book *Physikalische Hydrodynamik*. Actually Richardson's diagram places the storm tracks along the computed frontogenetic line given above, rather than along the deformation axis as indicated in the above reference. These two lines represent different things and do not necessarily have to follow each other closely. The deformation axis, is formed by the field of motion only, while the frontogenetic line is determined from the distribution of the frontogenetic function  $F$ , the product of  $|\nabla\alpha|$  and  $\phi$ , which has the real importance in determining the zone of frontal activity.

When the two are not coincident with each other, as is the case when the maximum  $|\nabla\alpha|$  zone does not fall along the deformation axis, or when the angle  $\phi$  is such that it does not give a large positive value of  $F$  along the axis, the actual frontal activity or the resultant cyclone tracks cannot coincide with the deformation axis of the field of motion. This is just what happens over the Pacific Ocean in the winter season when the cyclonic tracks and the deformation axis denoted in the *Physikalische Hydrodynamik* are quite widely separated. The characteristics and the real importance of a frontogenetic line are thus further established by this interesting example.



X.

ACKNOWLEDGEMENTS

The author wishes to express his thanks to Prof. Irving P. Krick, the Director of the Meteorological Department, Calif. Institute of Technology, Pasadena for his guidance in this research problem and suggestions in the preparation of the manuscript, and to Mr. Patrick Harney, graduate student of that Institute for his interest in proof reading the manuscript and discussing the material.

He also wishes to thank Dr. H.U. Sverdrup, the Director of the Scripps Institute of Oceanography, University of California, La Jolla, for his kindness in furnishing the Japanese Weather charts for extended use, and the Library of the U.S. Weather Bureau for loaning the author various articles pertinent to this study.

Final acknowledgement is due the China Foundation for the financial support which made the project possible.

REFERENCES


- (1) T. Bergeron, Uber die dreidimensional Verknupfende Wetteranalyse, Geofysiske Publikasjoner Vol.V, No.6, Oslo, 1928.
- (2) Literatures of the authors mentioned here listed in T. Bergeron's paper cited above. The author has read Ficker's papers of "Die Ausbreitung kalter Luft in Russland und Nordasien", Wien, 1910 and "Das Fortschreiten der Erwarmungen (der Warmewellen) in Russland und Nordasien", Wien, 1911.
- (3) Sverre Petterssen, Contribution to the Theory of Frontogenesis, Geofysiske Publikasjoner Vol. XI, No.6, Oslo, 1936.
- (4) Sverre Petterssen, Kinematical and Dynamical Properties of the Field of Pressure with Application to Weather Forecasting, Geof. Publ. Vol.X, No.2, Oslo, 1933.
- (5) W. Werenskiold, Mean monthly Air Transport over the North Pacific Ocean, Geofysiske Publikasjoner Vol.II, No. 9, 1922.
- (6) C.C. Chu, Circulation of Atmosphere over China, Memoir of the National Research Institute of Meteorology, Nanking, China, 1934.
- (7) C.C. Chu, A Brief Survey on the Climate of China, Memoir of the National Research Institute of Meteorology, Nanking, China, 1936.
- (8) E. Gherzi, Atlas Thermometrique de la Chine, Observatorie de Zi-Ka-Wei, Shanghai, China, 1934.
- (9) Pilot Chart of the North Pacific Ocean, Hydrographic Office of the Navy Department and the Weather Bureau, U. S. A.
- (10) Hsia-Chien Huang, Air Masses of North China, (not yet published).

- (11) W. Werenskiold, loc. cit. p. 16.
- (12) V. Bjerknes and others, Physikalische Hydrodynamik, 1933.
- (13) E. Gherzi, Air Masses acting over China and the adjacent Seas, Beitrage zur Physik der freien Atmosphäre, 24 Band, heft I, Leipzig, 1936.
- (14) H. C. Willet, American Air Mass Properties, M.I.T. Meteorological Papers, M.I.T., Cambridge, Mass., U.S.A., 1933.
- (15) V. Bjerknes and Others, loc. cit. p. 20.
- (16) C.C. Chu, loc. cit. p. 16. (Circulation of Atmosphere over China)
- (17) Sverre Petterssen, loc. cit. p. 2.
- (18) Shio-Wang Sung, The Extra-tropical Cyclones of the Eastern China and their characteristics, Memoir of the National Research Institute of Meteorology, Nanking, China, 1931.
- (19) C.C. Chu, loc. cit. p. 16. (Circulation of Atmosphere over China)
- (20) V. Bjerknes and others, loc. cit. p. 20.
- (21) C.C. Chu, loc. cit. p. 16. (Circulation of Atmosphere over China)
- (22) V. Bjerknes and others, loc. cit. p. 20.
- (23) Sverre Petterssen, loc. cit. p. 2.
- (24) Gerhart Schinze, Die praktische Wetteranalyse, Hamburg, 1932.
- (25) N.V. Stremoussov, About the Synoptic process in the Eastern Part of the Asiatic Continent and the Adjacent Seas, Jn. of Geophysics, Vladivostok, Dec. 1934.
- (26) Bulletin of the American Meteorological Society, Vol.17, No.10, October, 1936.

- (27) V. Bjerknes and others, loc. cit. p. 20.
- (28) Robert W. Richardson, Winter Air Mass Convergence over the North Pacific, Monthly Weather Review, June 1936.

EXPLANATION OF SYMBOLS USED ON SYNOPTIC CHARTS

Unless otherwise indicated, the charts are for the observations of 12 noon, 120°E Standard Time.

○	Clear
◐	Partly cloudy
●	Overcast
:●	Raining
*●	Snowing
////	Intermittent rain area
▽	Shower
	Rain area
▲▲▲	Cold front
●●●	Warm front
▲●●●	Occluded front

Air mass symbols are as given in the text.

Number of barbs on wind arrows gives velocity in Beaufort Scale.

One half barb represents one Beaufort unit, and each full barb two Beaufort units.

Pressures in mm. are given to the upper right of the station, and temperatures in degrees Centigrade to the lower right of the station.

CHART I

DEFORMATION FIELD AND ISOTHERM CHART  
APRIL

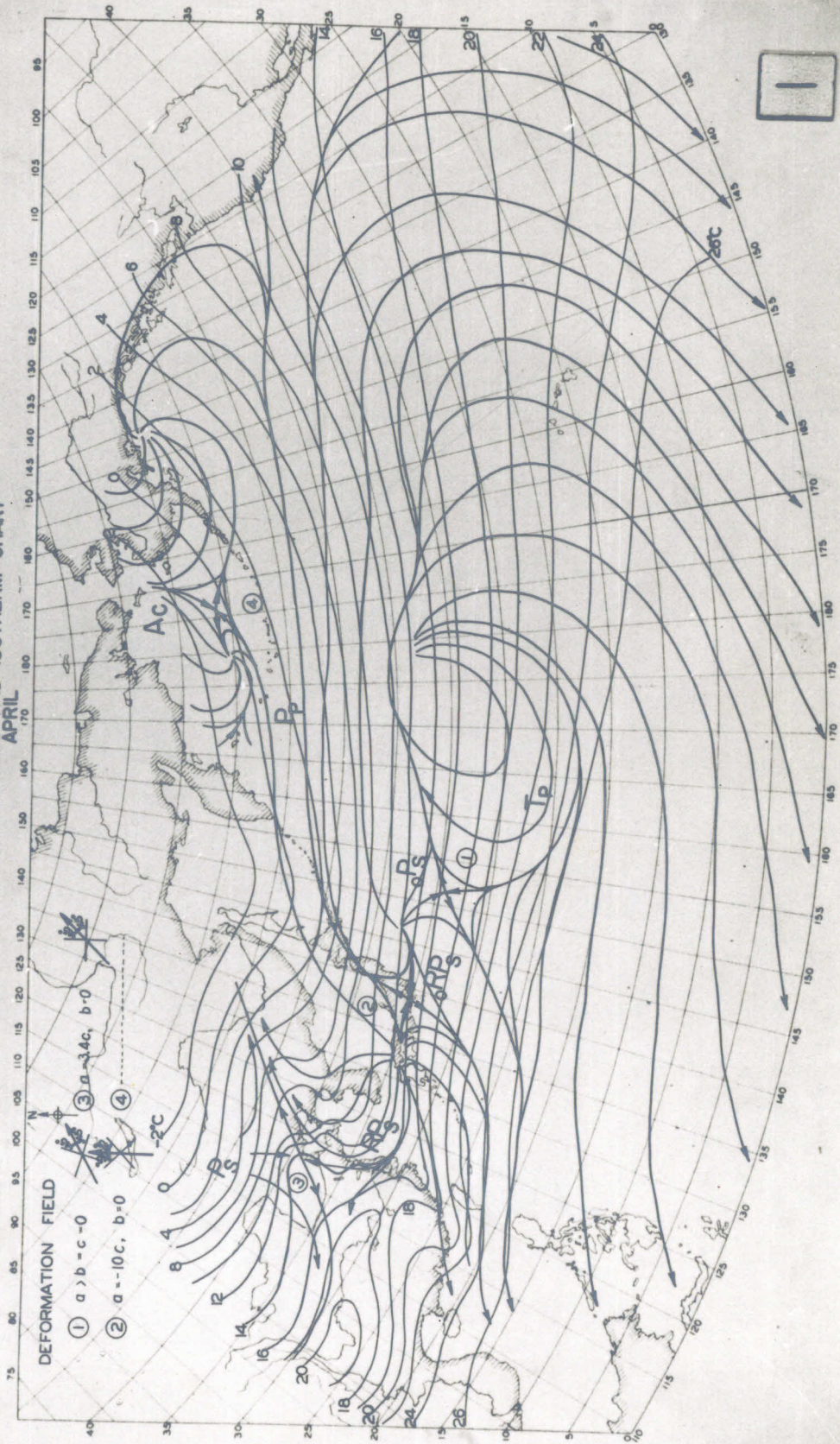


CHART II

WIND DIRECTIONS OVER CHINA  
APRIL

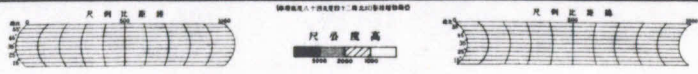
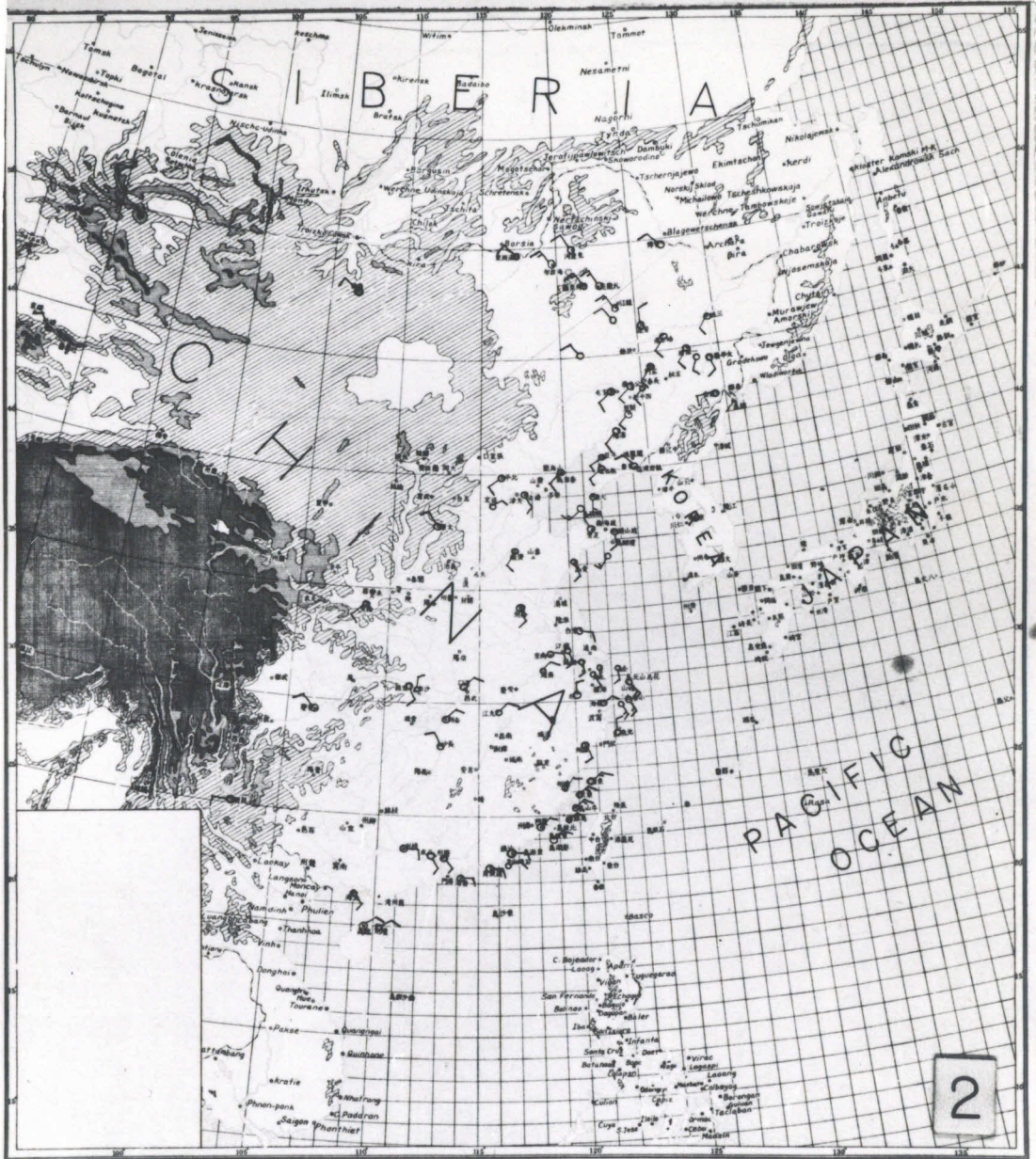


CHART III  
 $|\nabla\alpha|$  FIELD IN THE FAR EAST  
APRIL

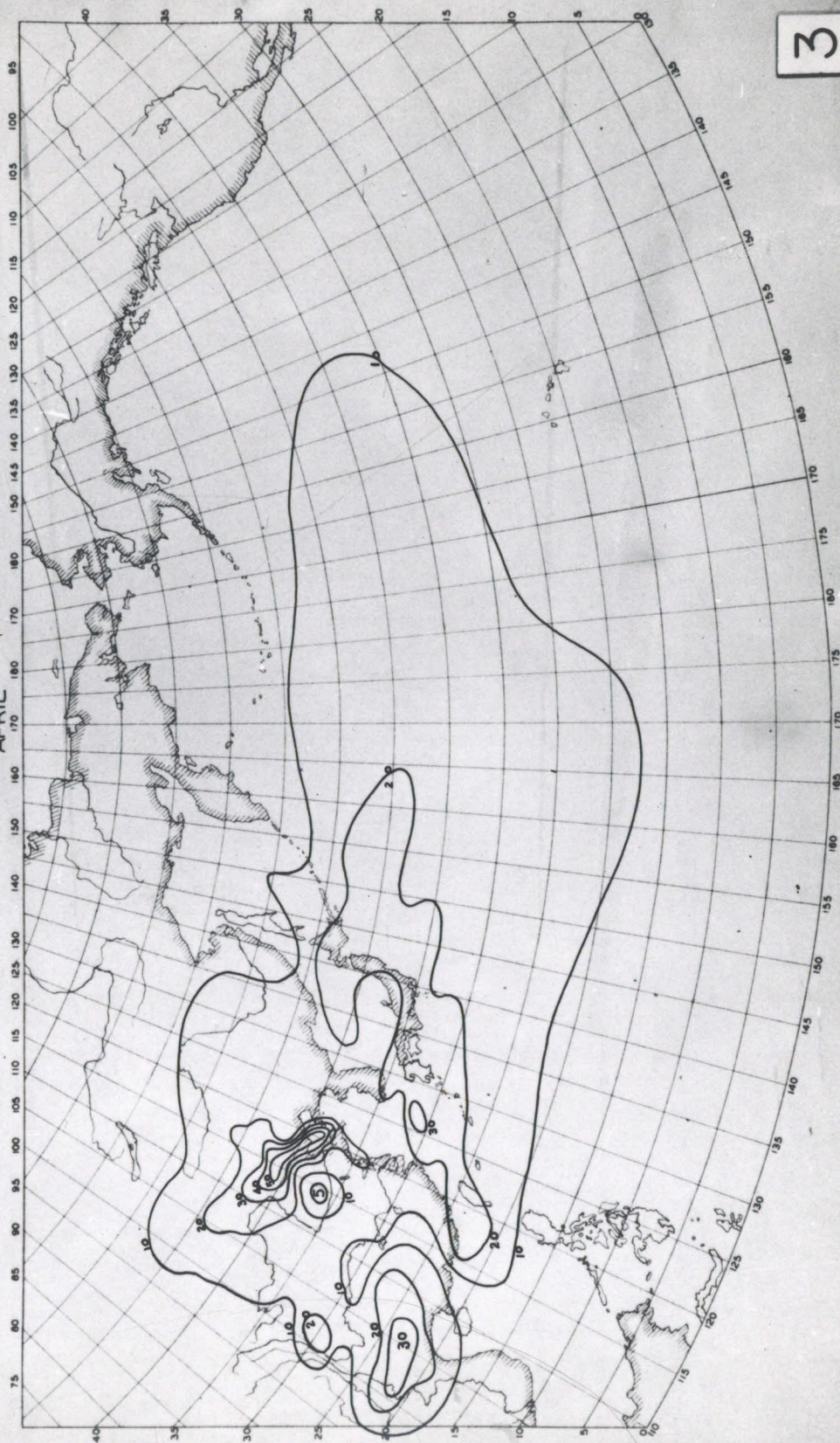
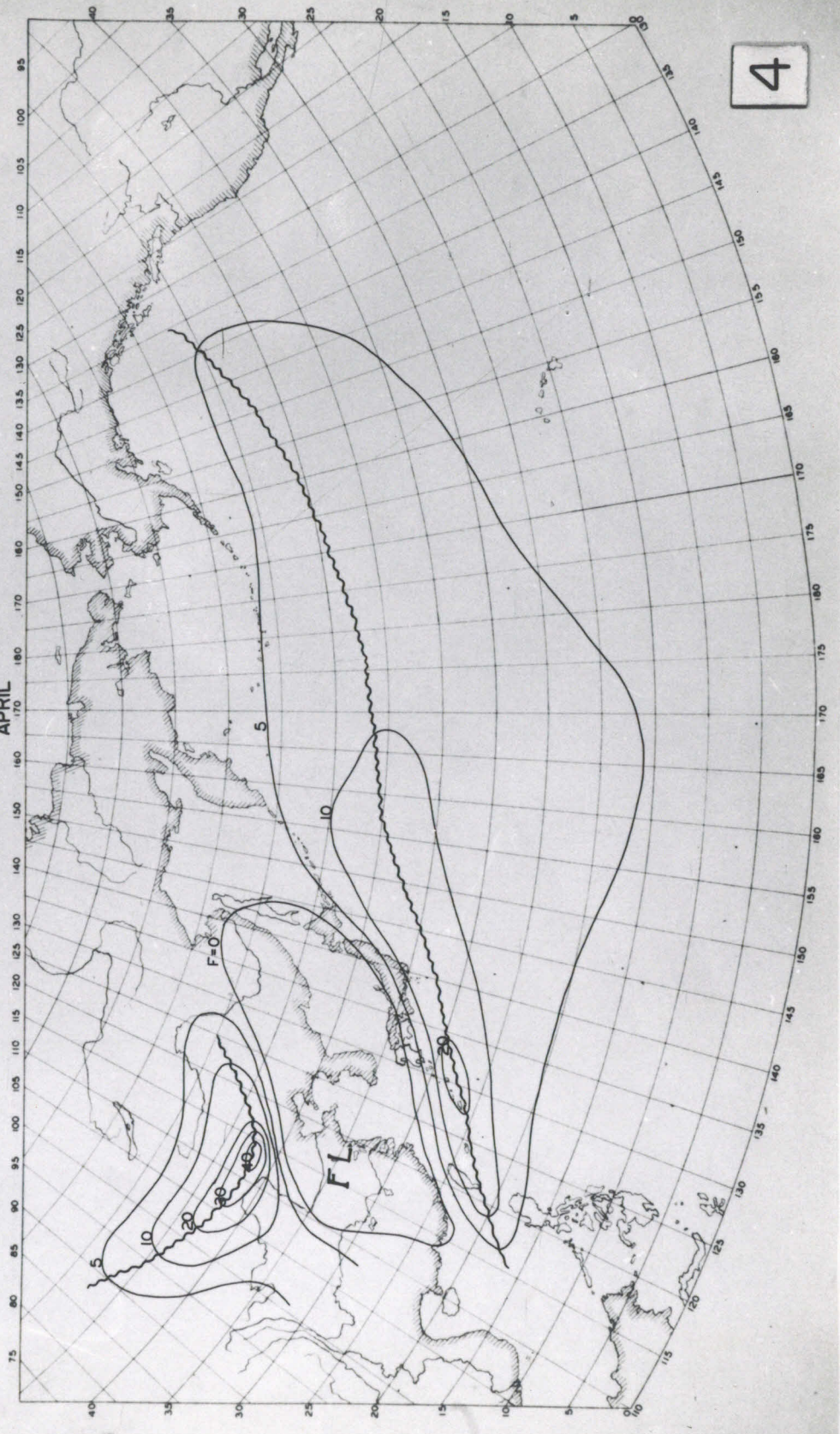


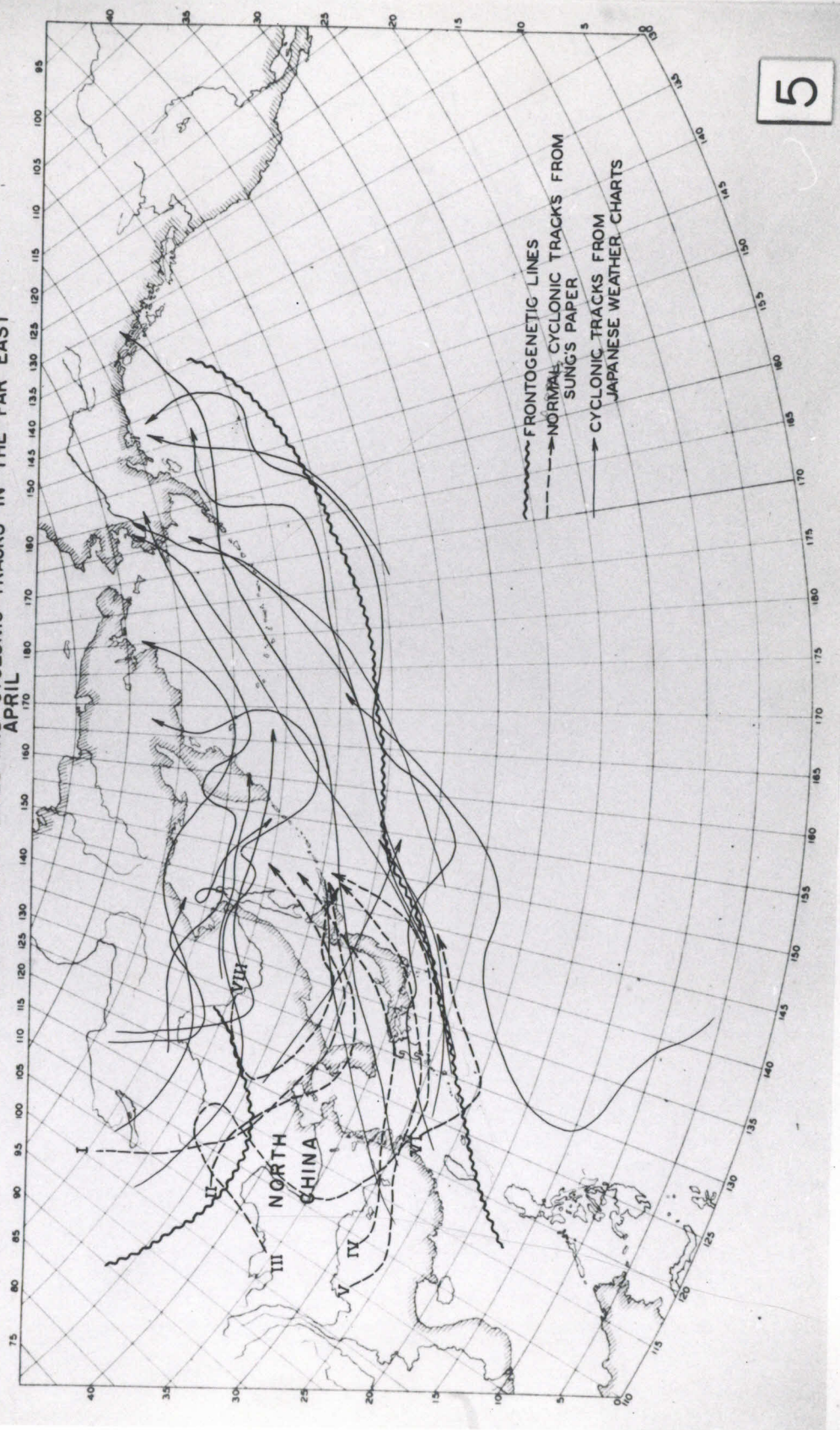


CHART IV  
DISTRIBUTION OF F IN THE FAR EAST  
APRIL



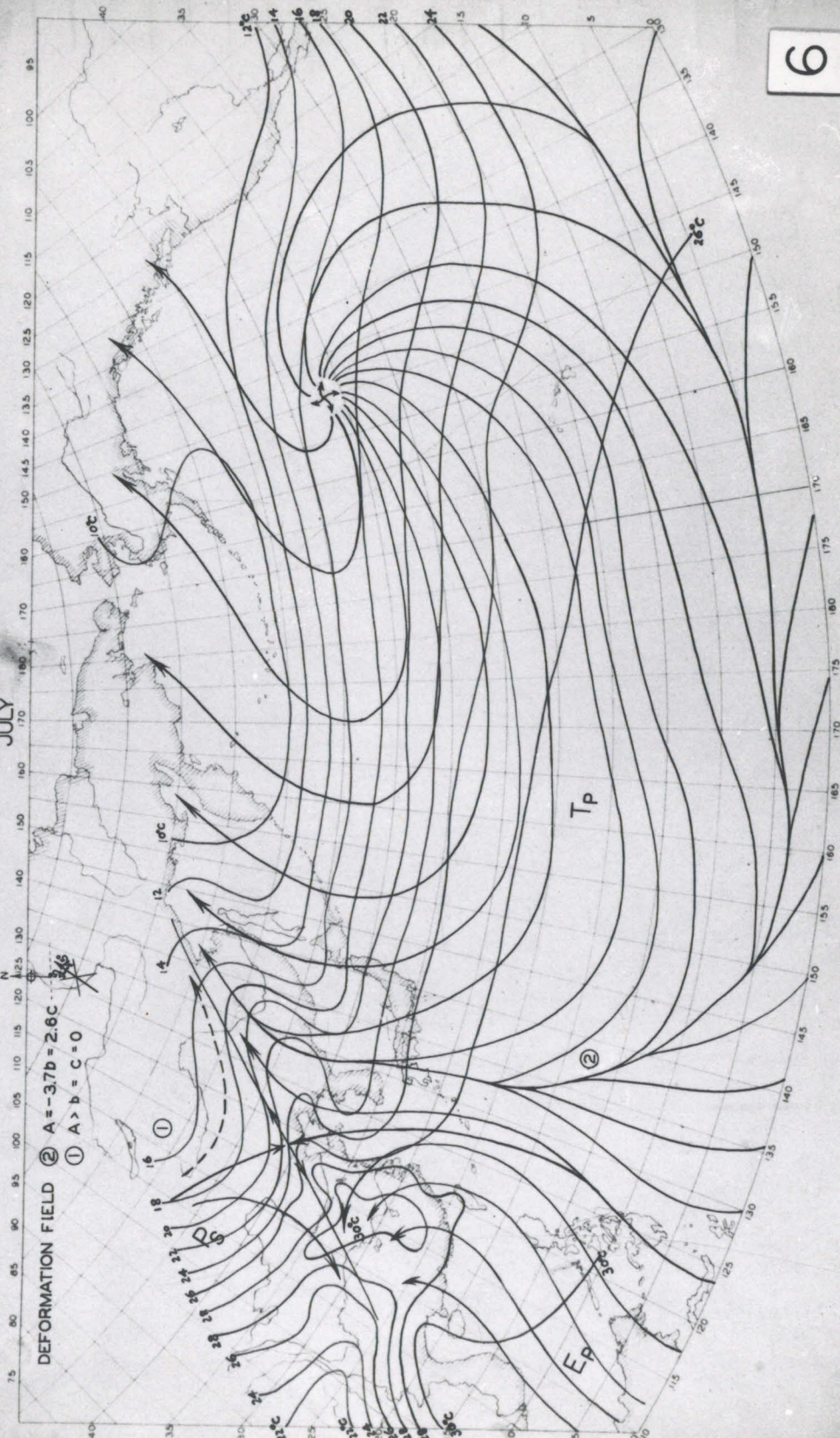
FRONTOGENETIC LINES AND CYCLONIC TRACKS IN THE FAR EAST  
APRIL

CHART V



DEFORMATION FIELD AND ISOTHERM CHART  
JULY

CHART VI



DEFORMATION FIELD ②  $A = -3.7b = 2.6C$   
①  $A > b = C = 0$

6

FIELD IN THE FAR EAST  
JULY

CHART VII

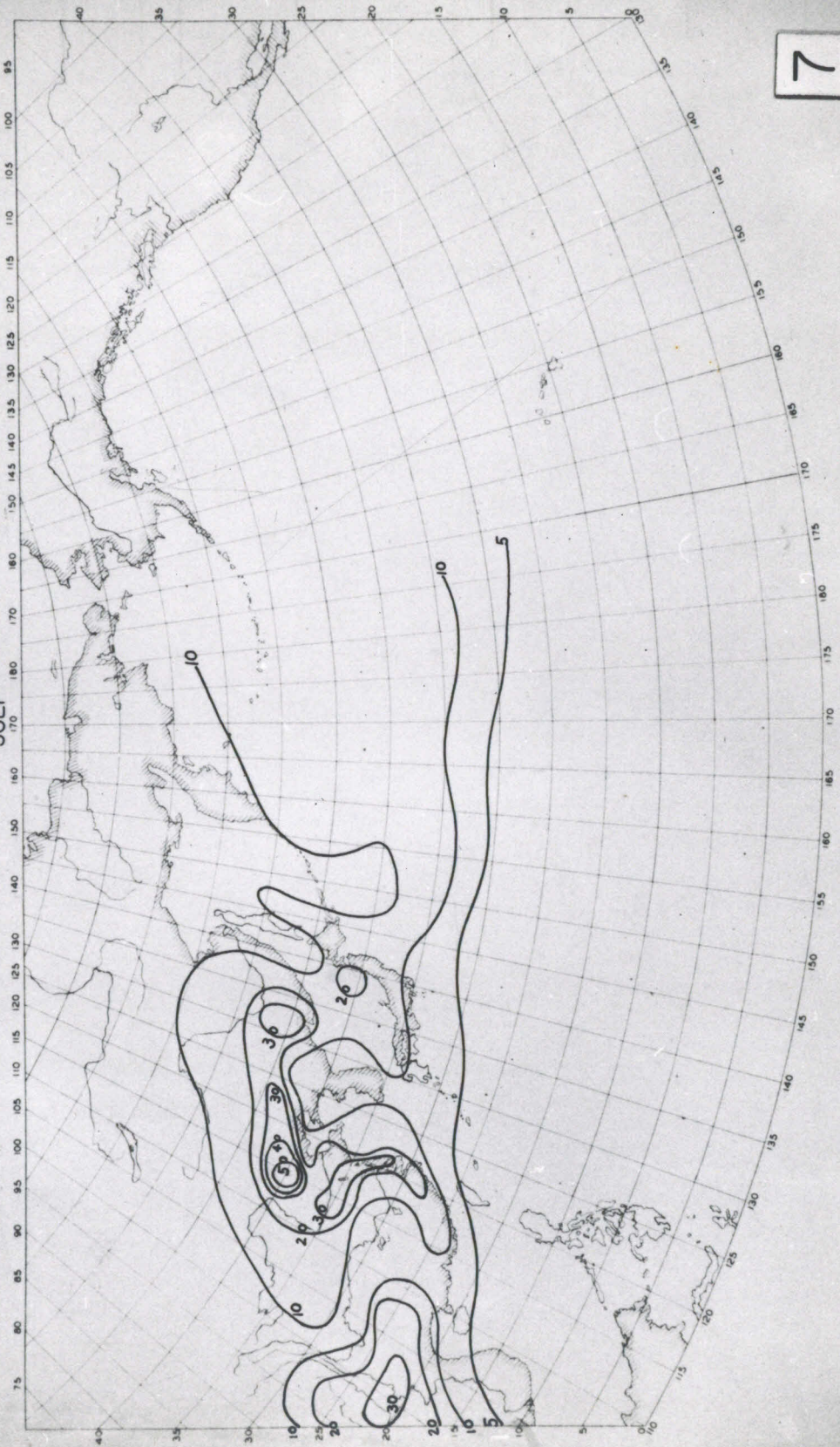


CHART VIII

DISTRIBUTION OF F IN THE FAR EAST

JULY

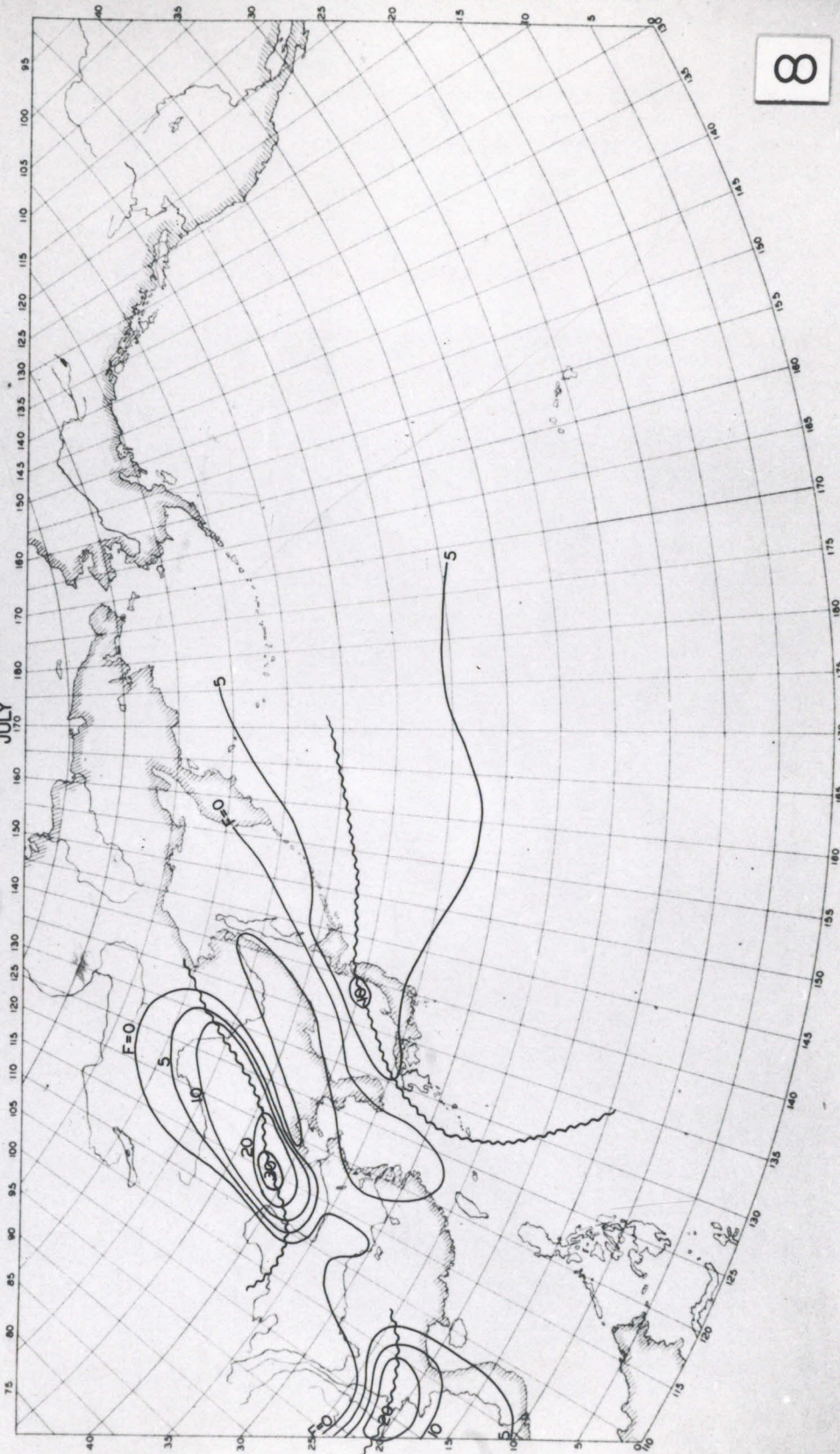


CHART IX

FRONTOGENETIC LINES AND CYCLONIC TRACKS IN THE FAR EAST  
JULY

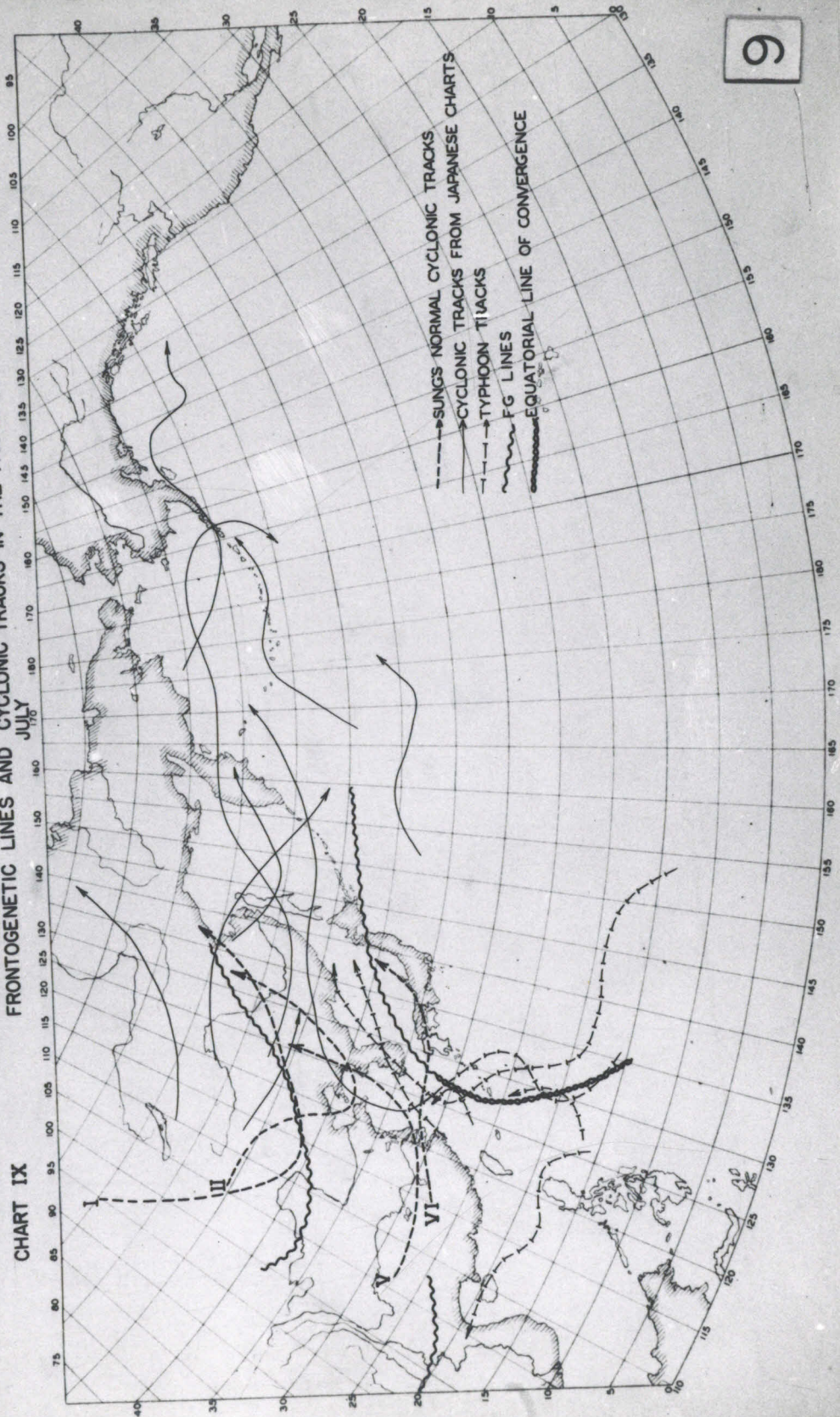
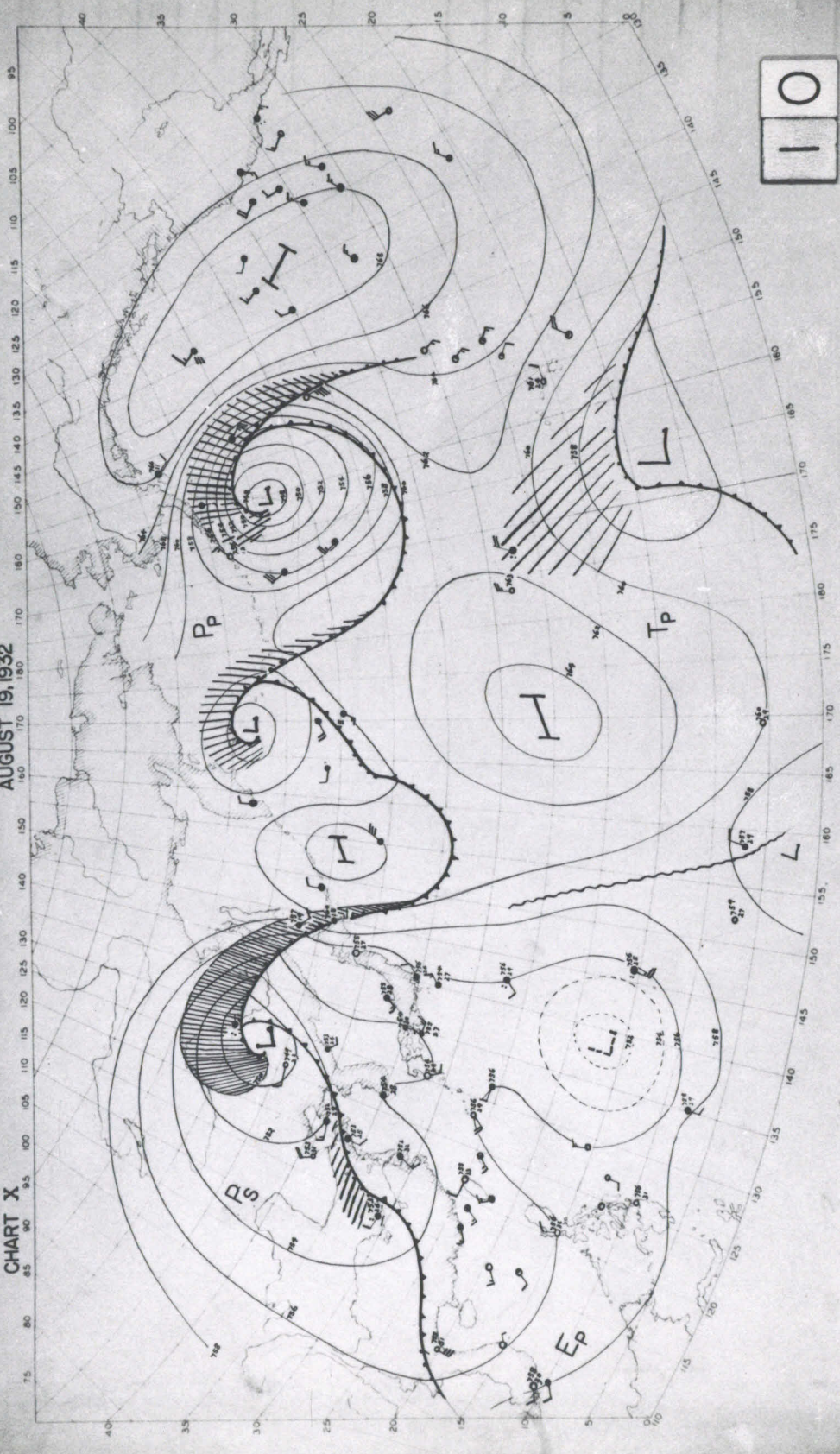


CHART X

AUGUST 19, 1932



110

CHART XI

AUGUST 20, 1932

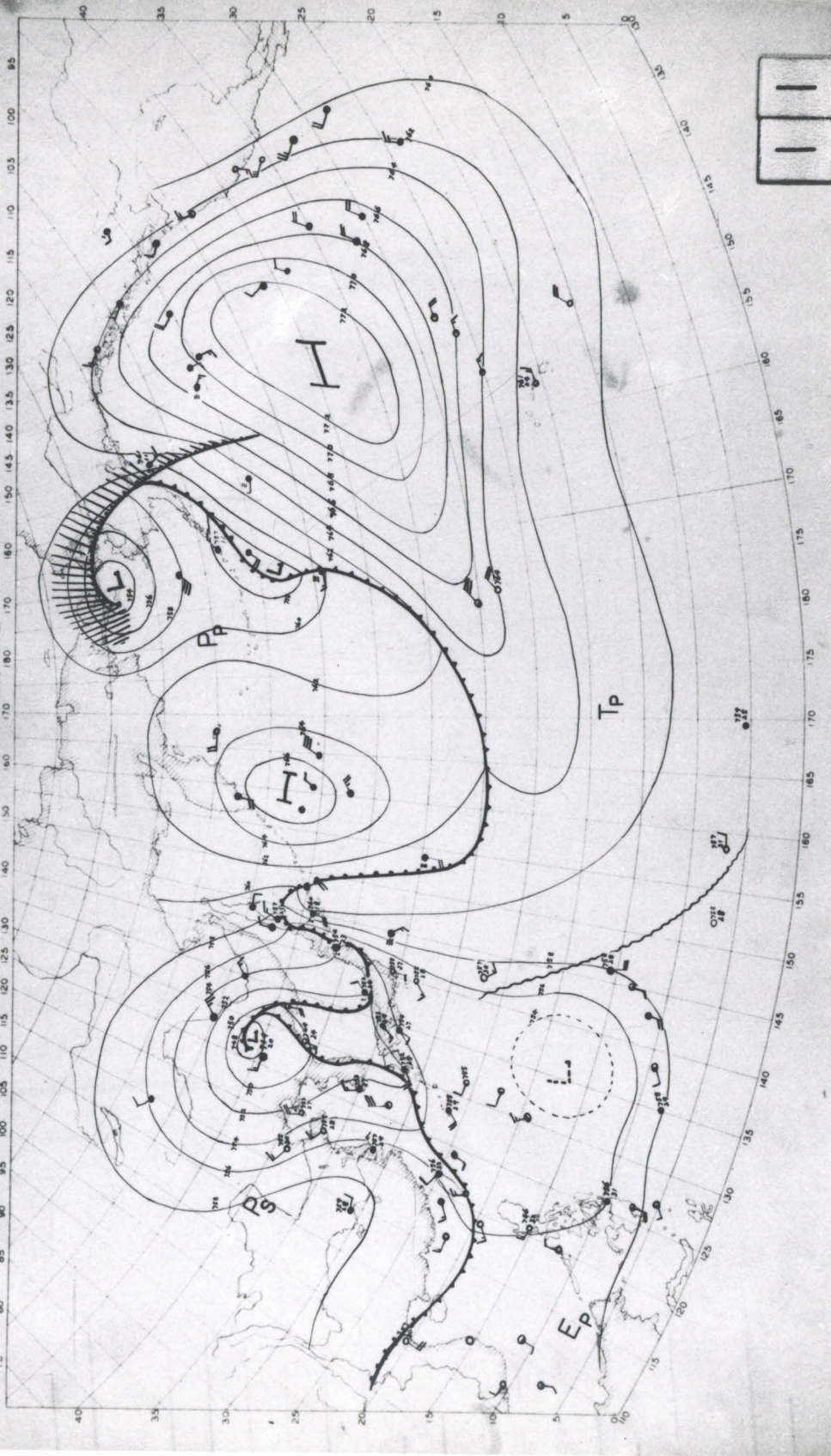




CHART XII

AUGUST 21, 1932

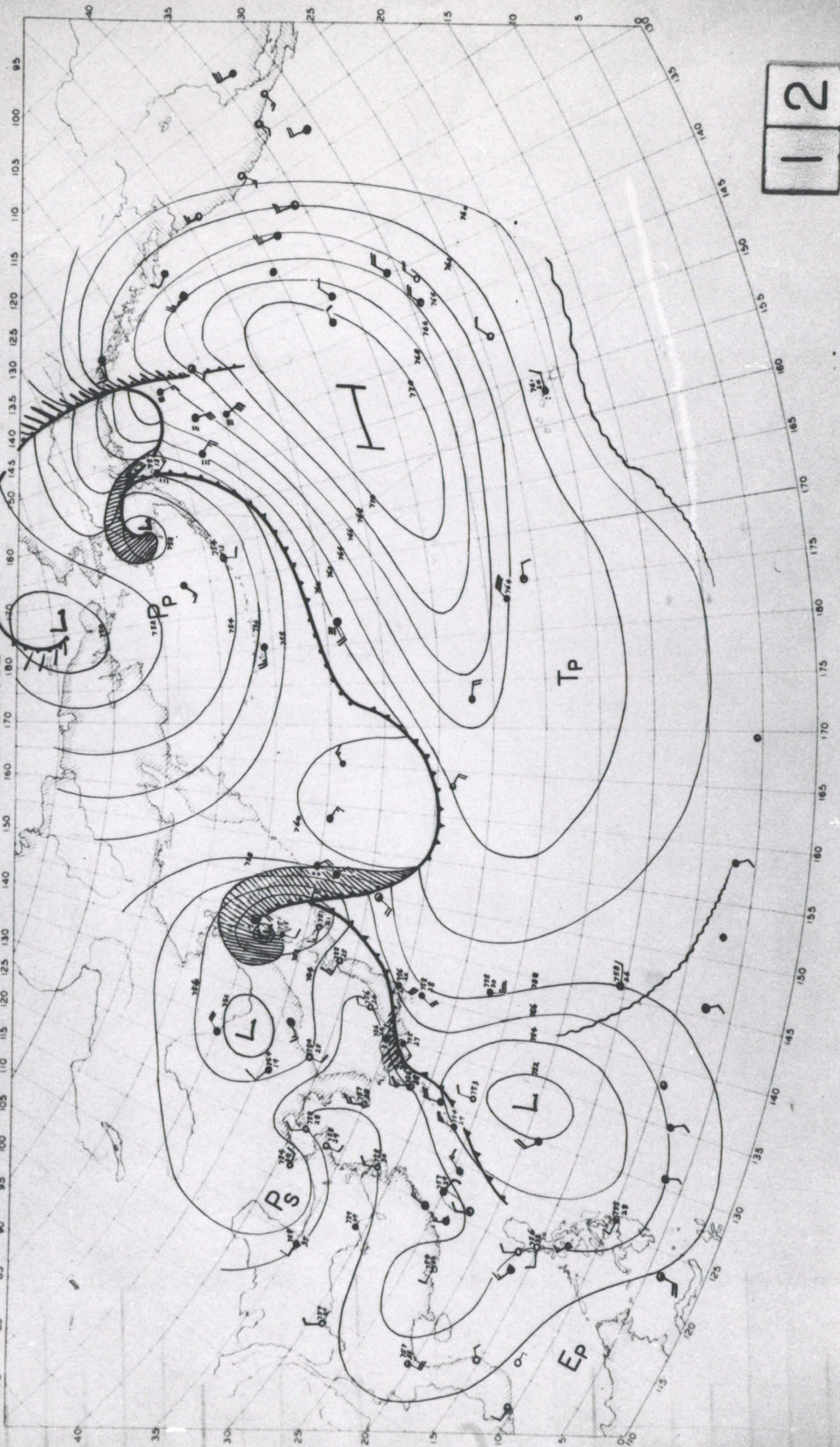
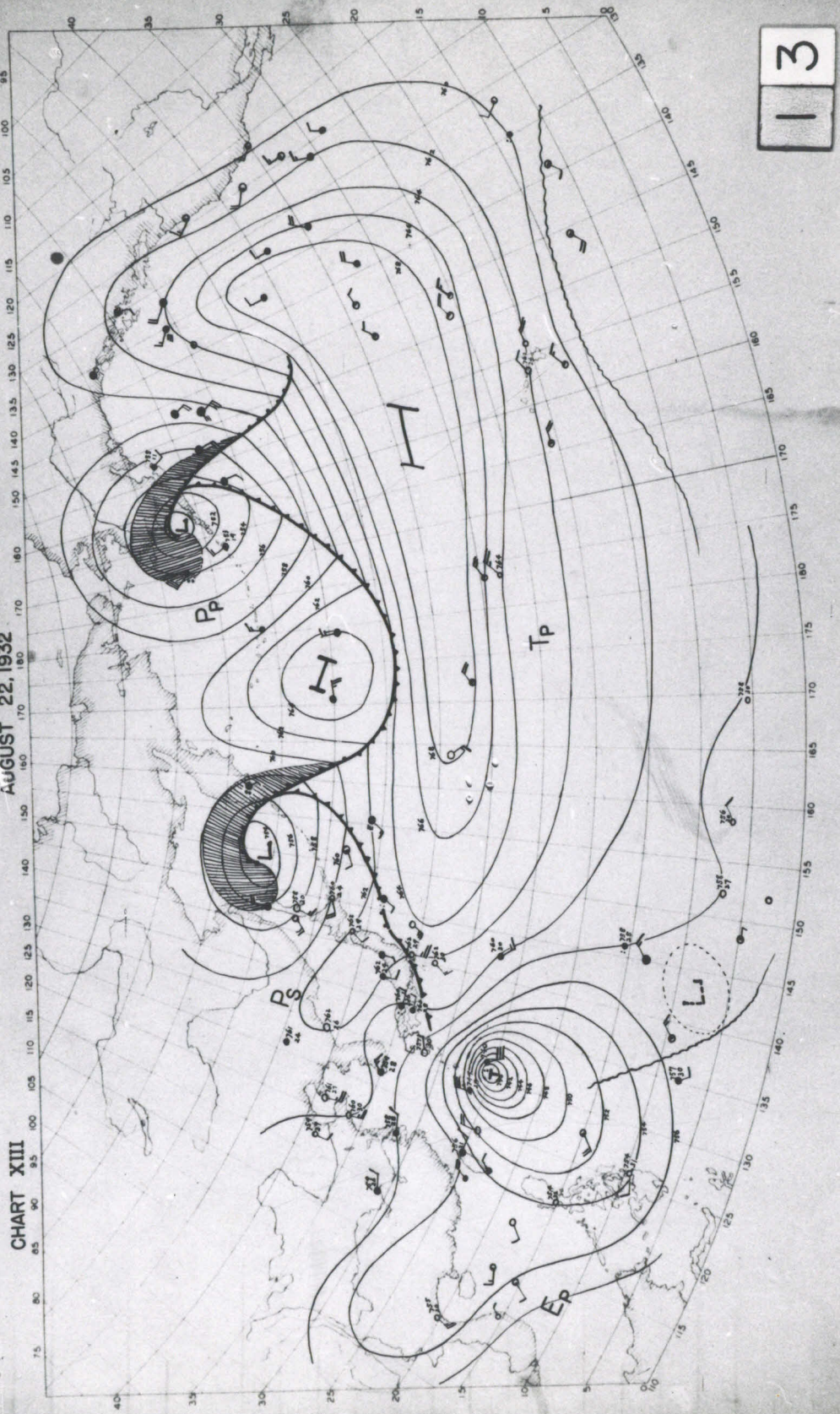


CHART XIII

AUGUST 22, 1932



13

DEFORMATION FIELD AND ISOTHERM CHART  
SEPTEMBER

CHART XIV

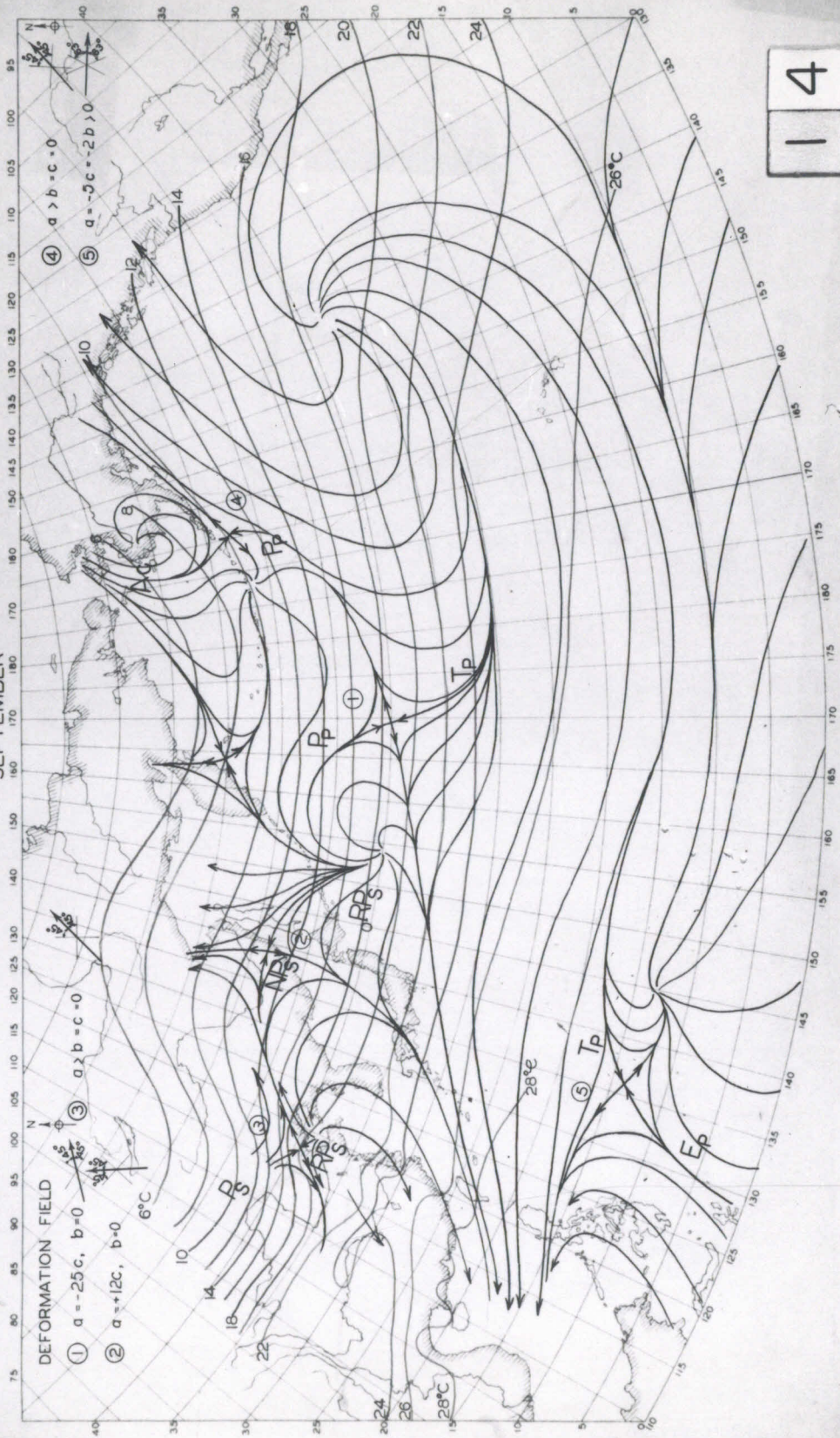


CHART XV

$|\Delta\alpha|$  FIELD IN THE FAR EAST  
SEPTEMBER

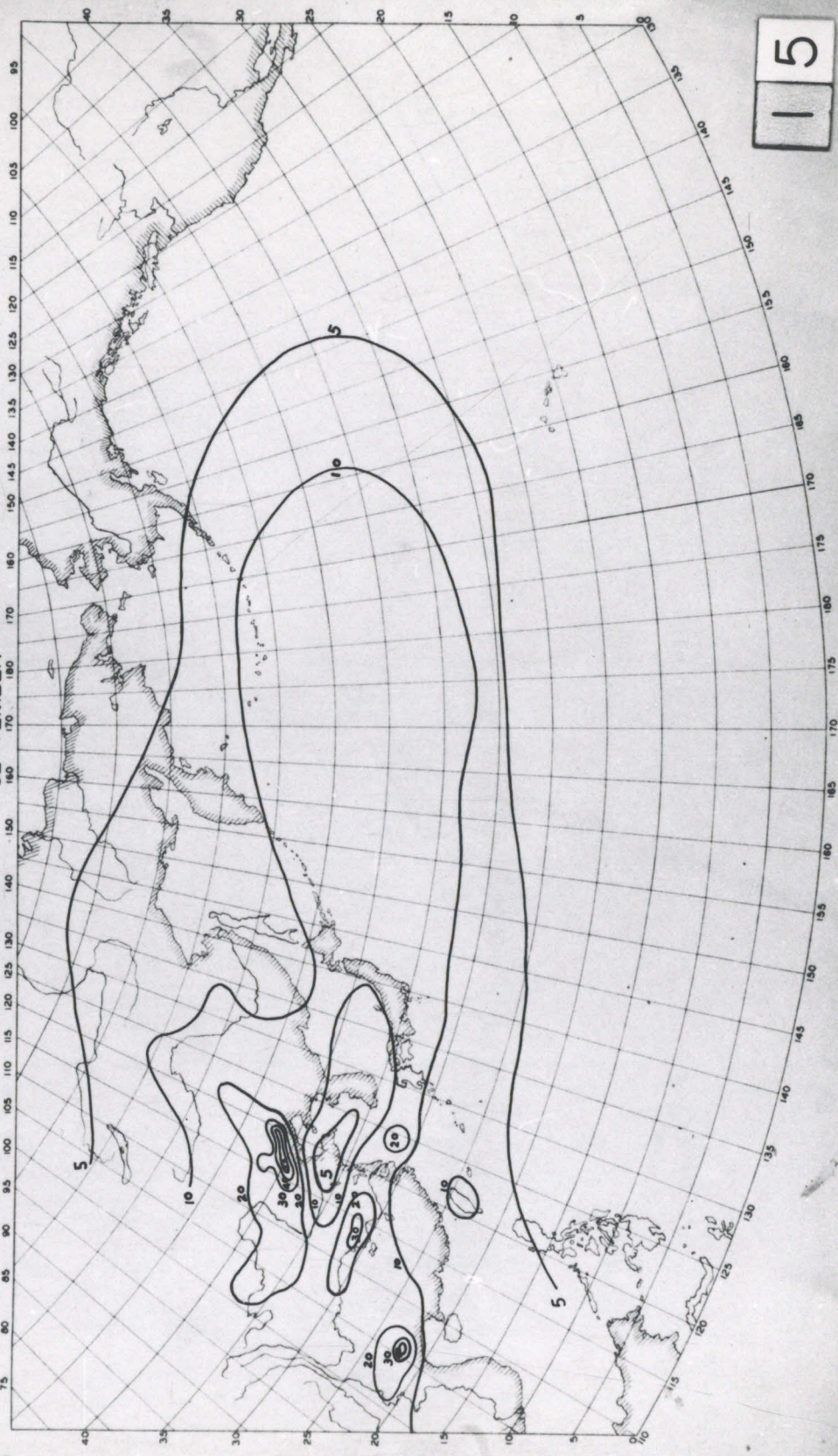
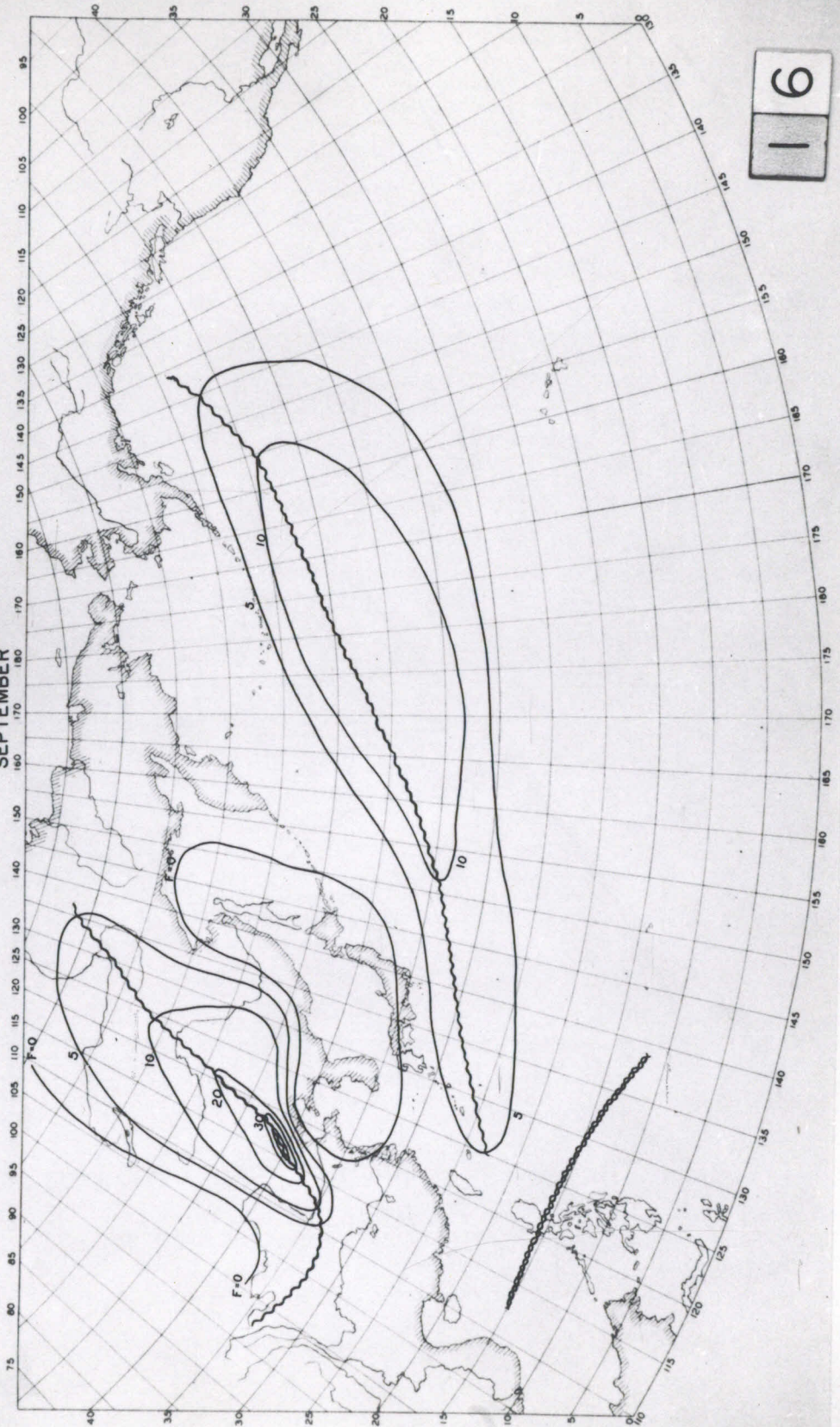


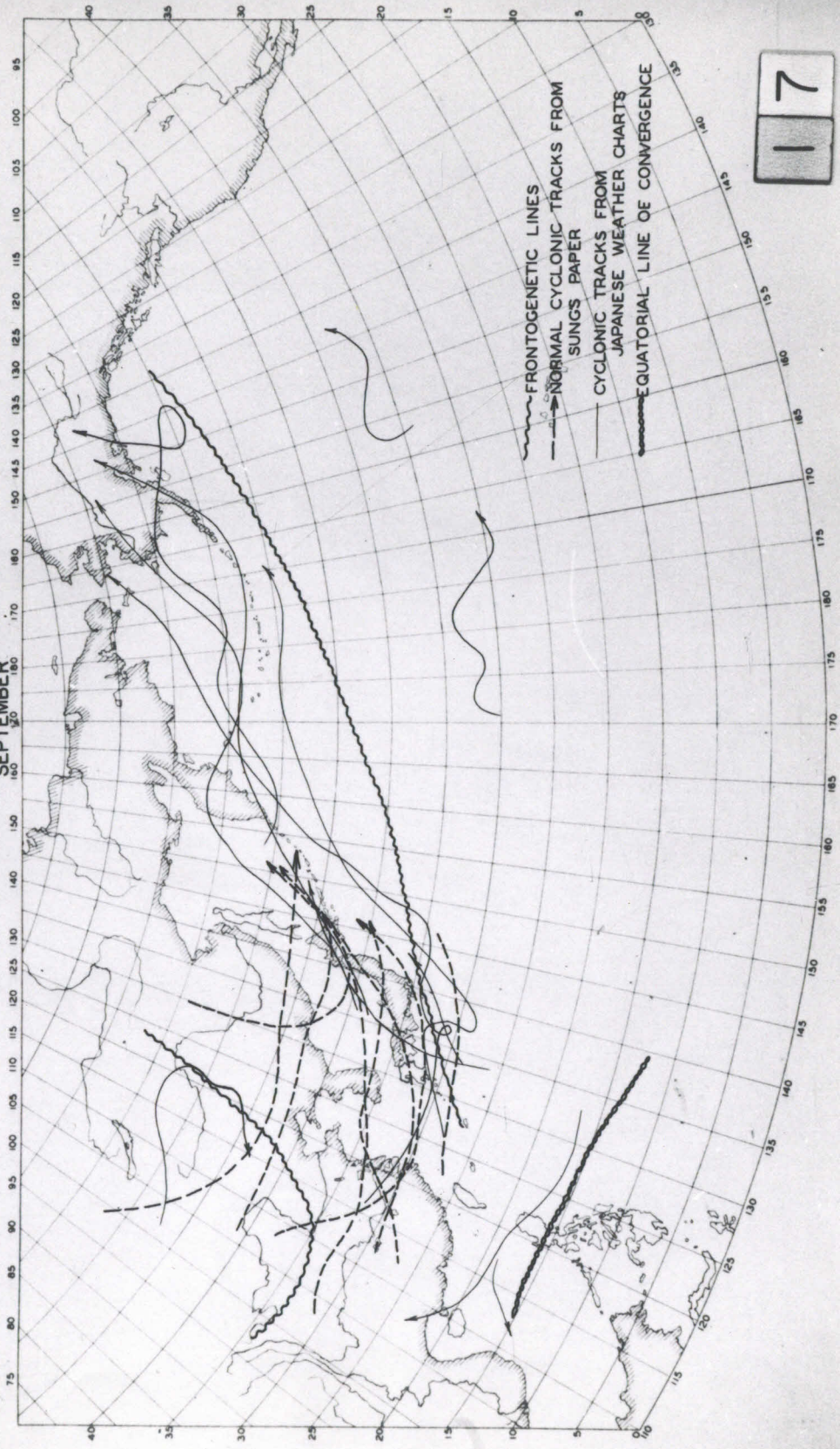
CHART XVI

DISTRIBUTION OF F IN THE FAR EAST  
SEPTEMBER



FRONTOGENETIC LINES AND CYCLONIC TRACKS IN THE FAR EAST  
SEPTEMBER

CHART XVII



117

CHART XVIII DEFORMATION FIELD AND ISOTHERM CHART JANUARY

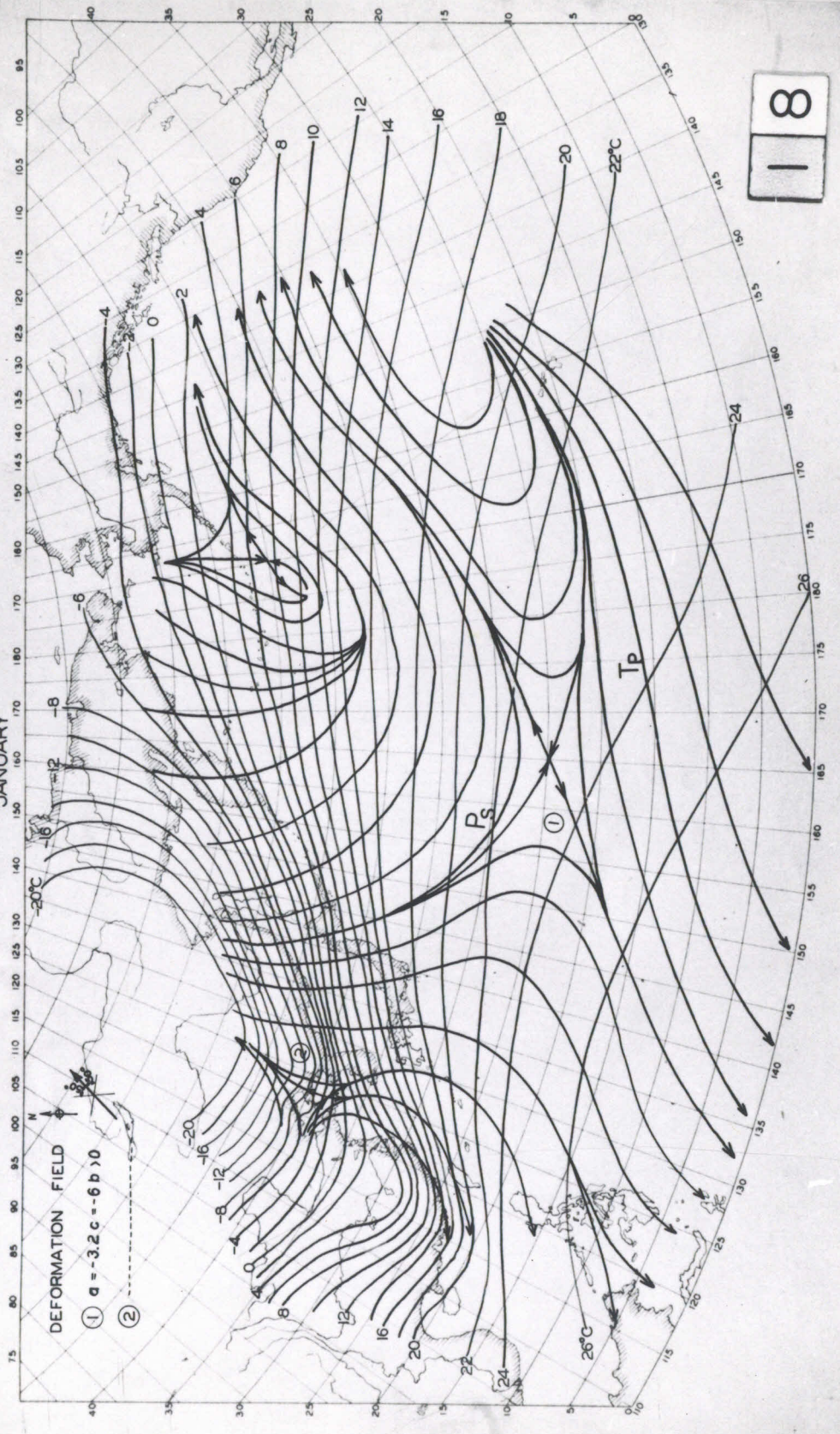


CHART XVIII

DEFORMATION FIELD

- ①  $a = -3.2c - 6b > 0$
- ②

118

CHART XIX  
FIELD IN THE FAR EAST  
JANUARY

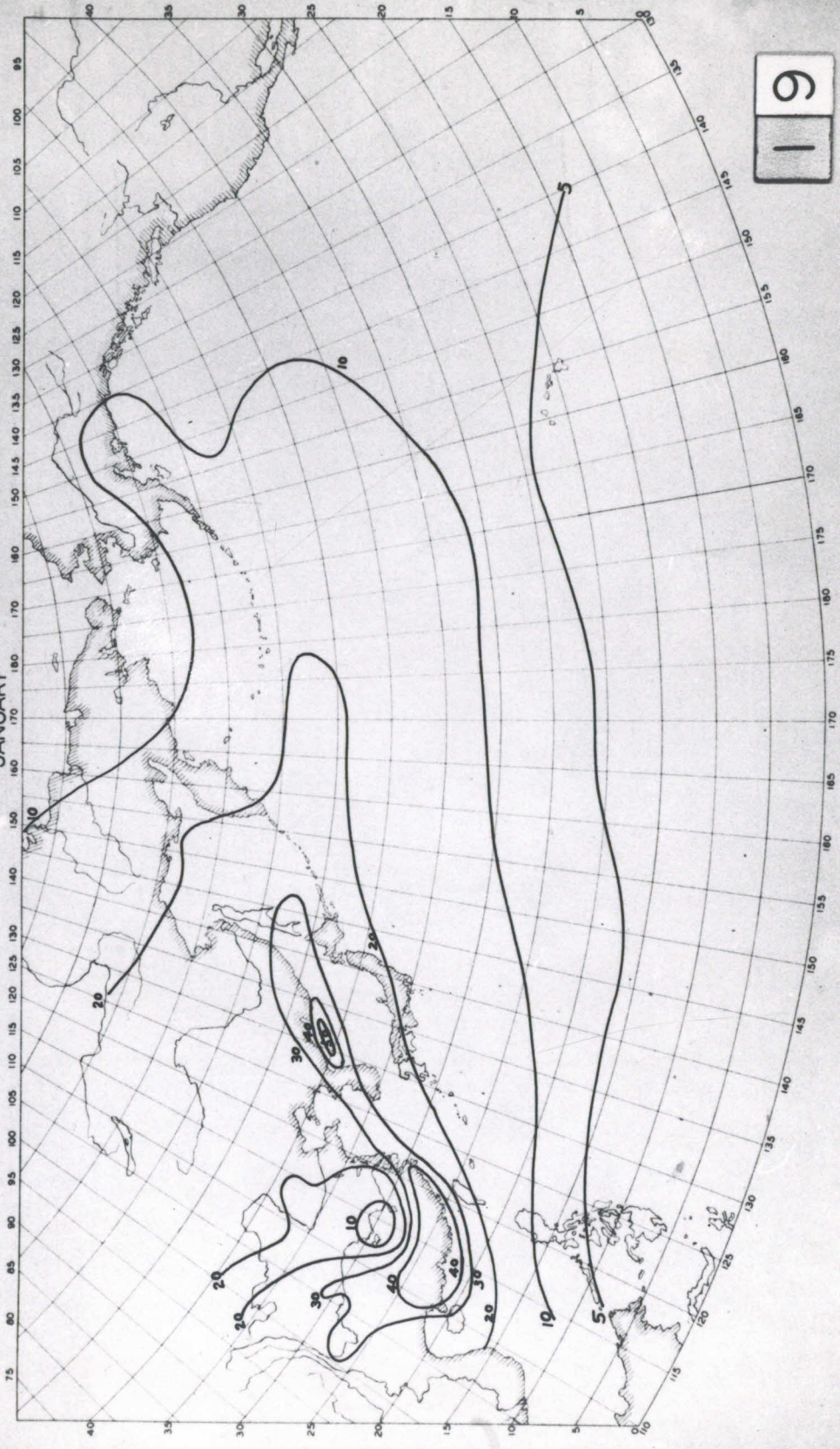
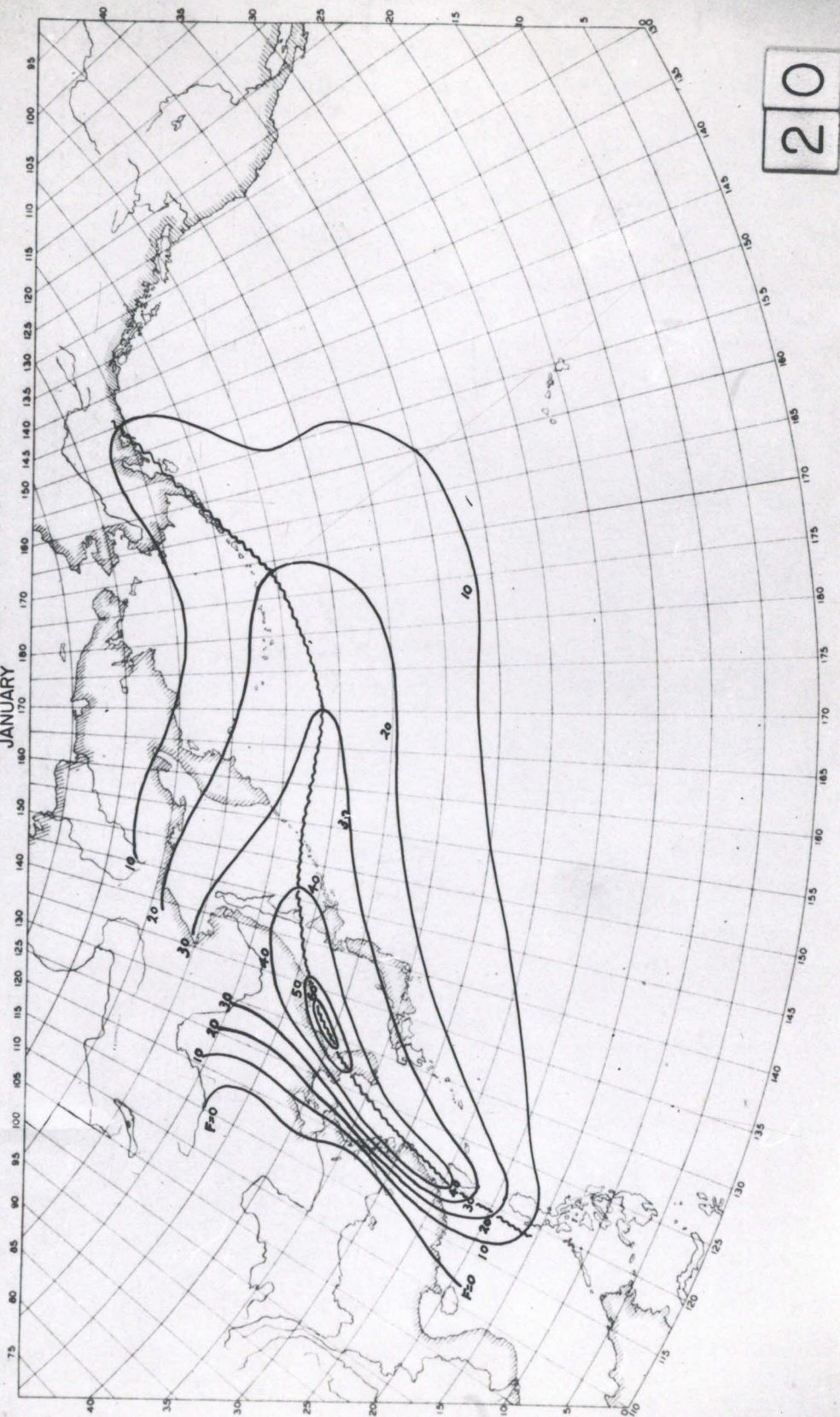




CHART XX

DISTRIBUTION OF F IN THE FAR EAST  
JANUARY



20

FRONTOGENETIC LINE AND CYCLONIC ACTIVITY  
JANUARY

CHART XXXI

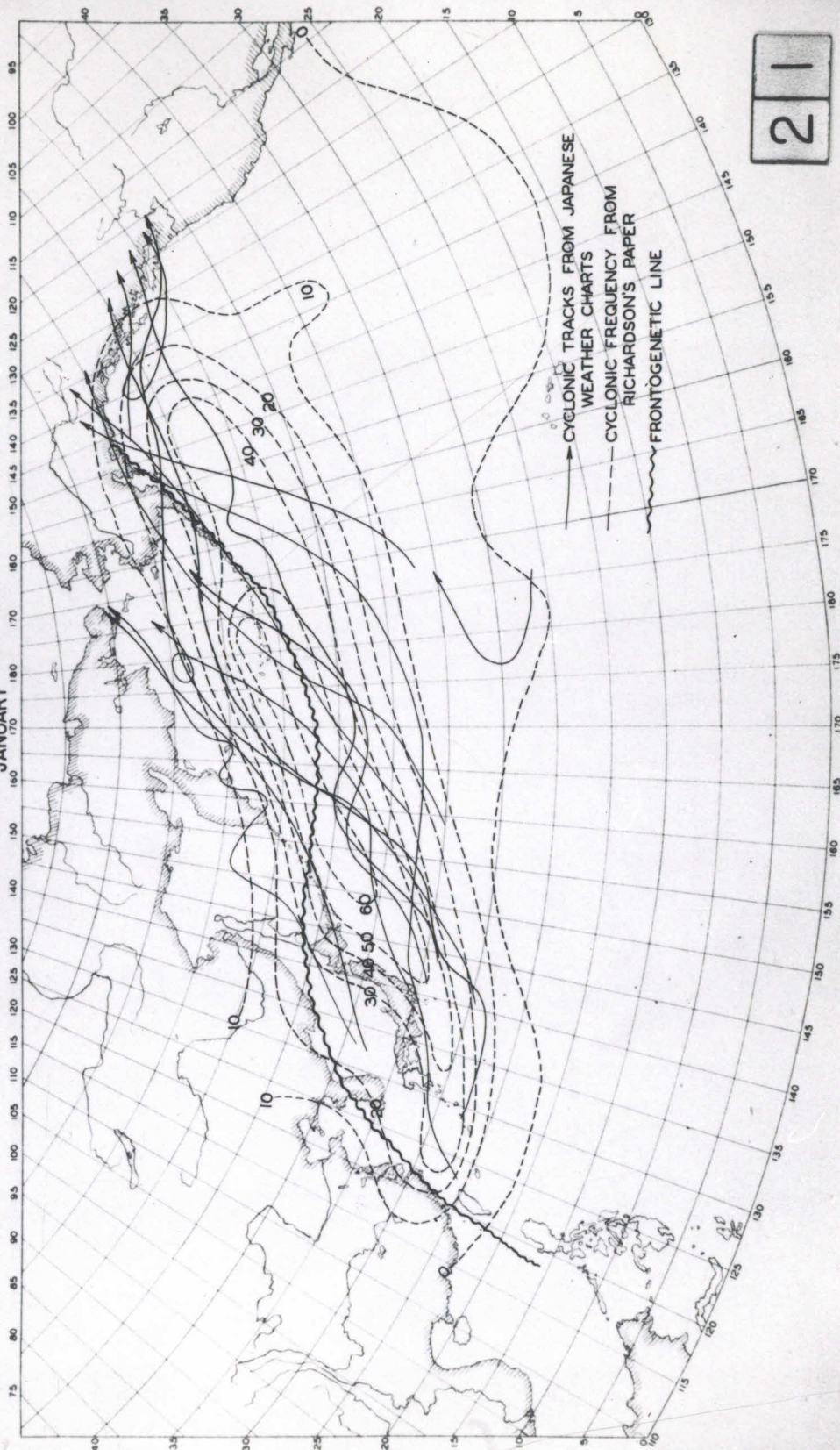
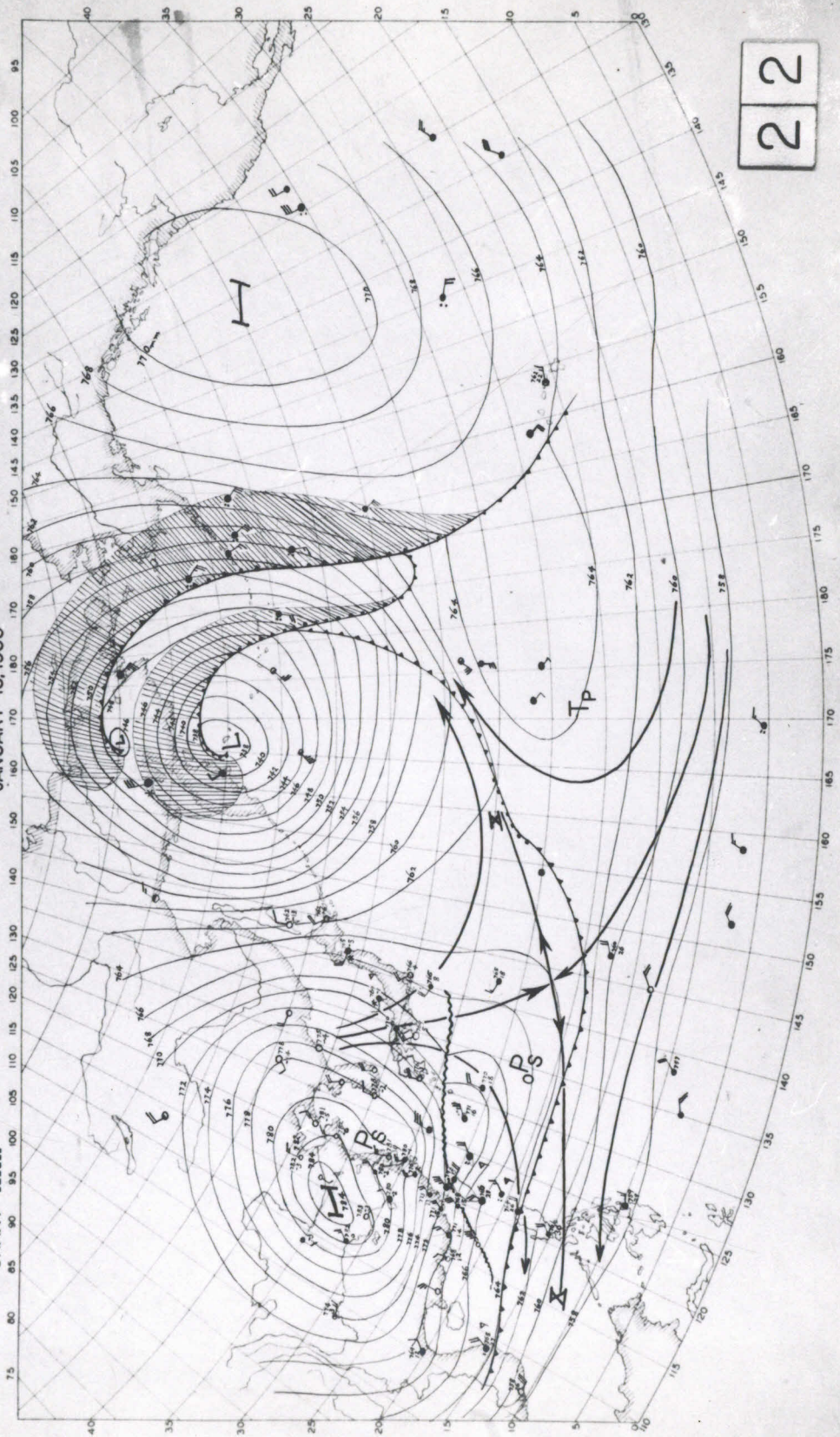


CHART XXII

JANUARY 15, 1933



22

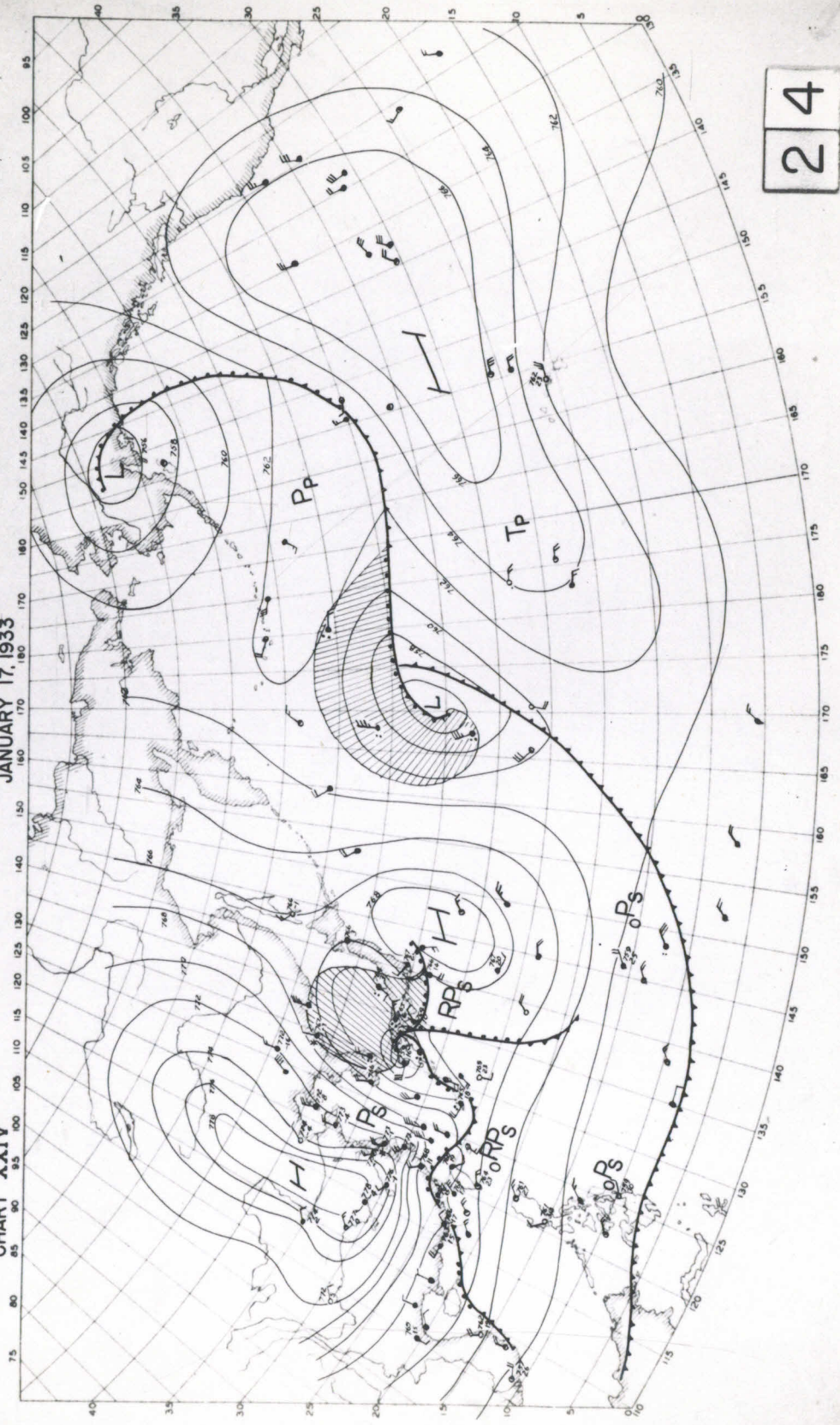
CHART XXIII

JANUARY 16, 1933



CHART XXIV

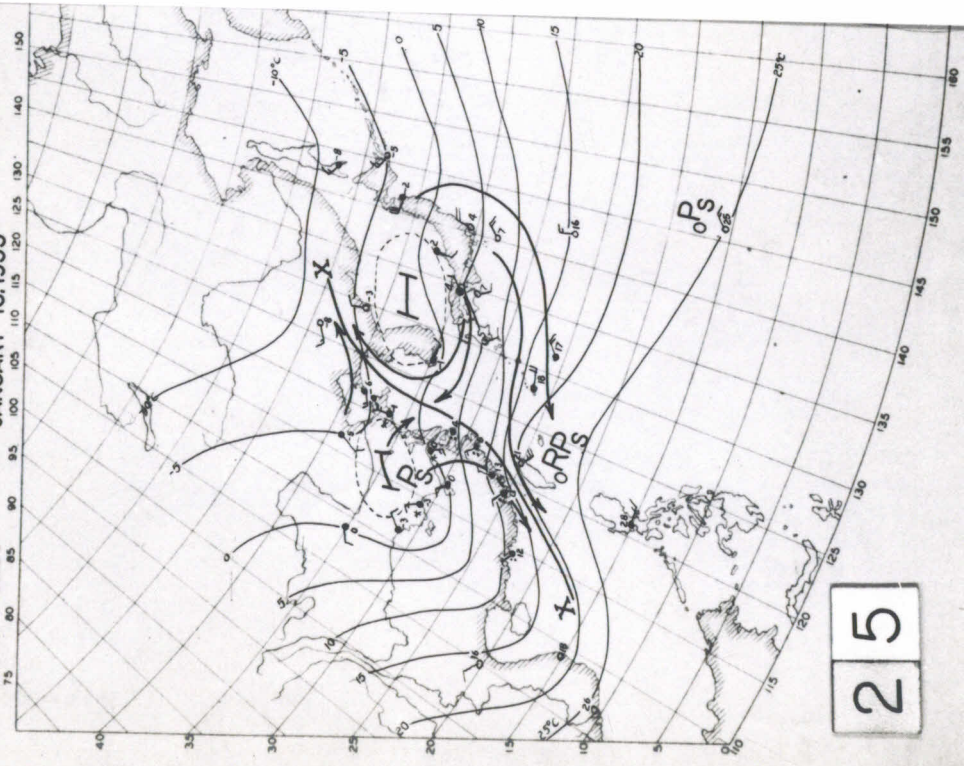
JANUARY 17, 1933



24

CHART XXV

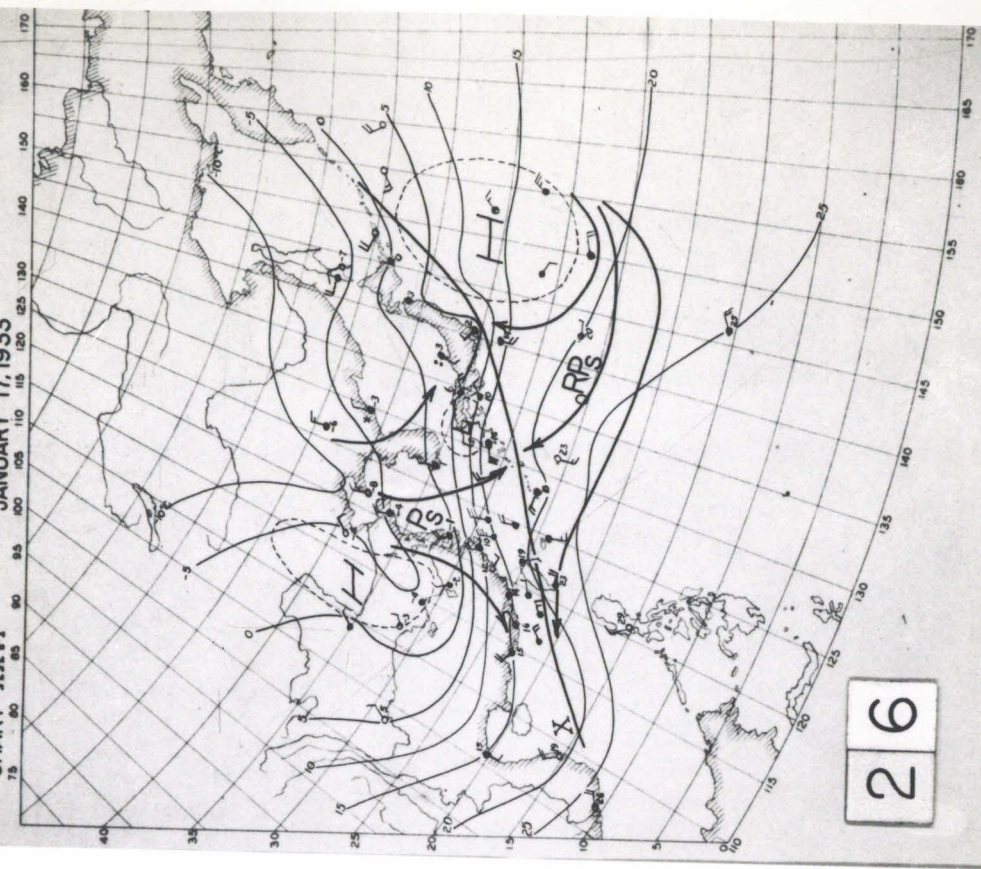
JANUARY 16, 1933



25

CHART XXVI

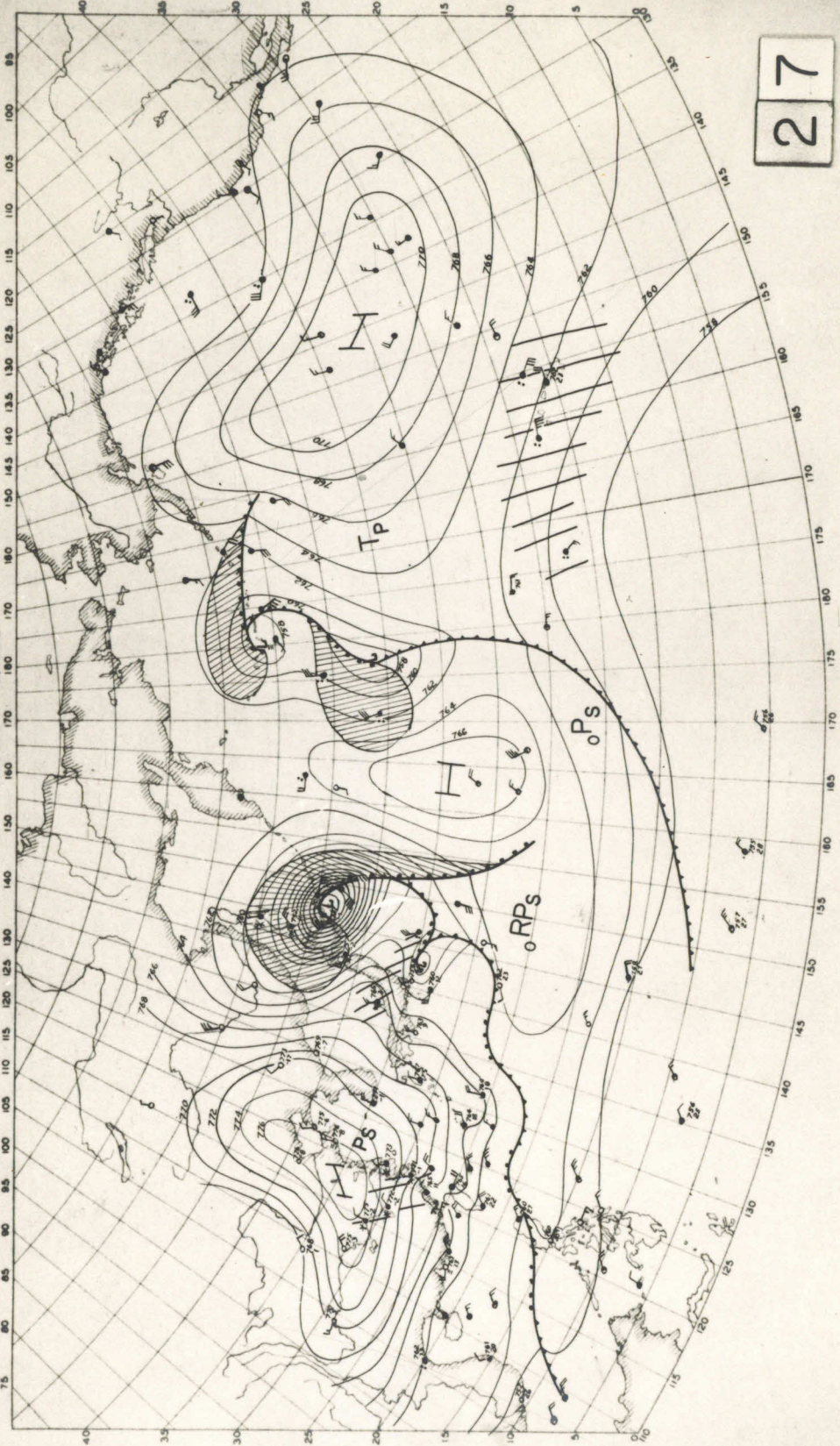
JANUARY 17, 1933



26

CHART XXVII

JANUARY 18, 1933



27